

The changing hydrology of an irrigated and dammed Yangtze River: streamflow, extremes, and lake hydrodynamics

Haoran Hao, Ningpeng Dong, Mingxiang Yang, Jianhui Wei, Xuejun Zhang, Shiqin Xu, Denghua Yan, Liliang Ren, Guoyong Leng, Lu Chen, Xudong Zhou, Hao Wang, Lijuan Song, Harald Kunstmann

Angaben zur Veröffentlichung / Publication details:

Hao, Haoran, Ningpeng Dong, Mingxiang Yang, Jianhui Wei, Xuejun Zhang, Shiqin Xu, Denghua Yan, et al. 2024. "The changing hydrology of an irrigated and dammed Yangtze River: streamflow, extremes, and lake hydrodynamics." *Water Resources Research* 60 (10): e2024WR037841.
<https://doi.org/10.1029/2024wr037841>.

Water Resources Research®












RESEARCH ARTICLE

10.1029/2024WR037841

Haoran Hao and Ningpeng Dong
contributed equally to this work.

The Changing Hydrology of an Irrigated and Dammed Yangtze River: Streamflow, Extremes, and Lake Hydrodynamics

Haoran Hao^{1,2}, Ningpeng Dong^{2,3} , Mingxiang Yang², Jianhui Wei⁴ , Xuejun Zhang² ,
Shiqin Xu⁵ , Denghua Yan² , Liliang Ren³ , Guoyong Leng⁶, Lu Chen⁷ , Xudong Zhou⁸ ,
Hao Wang², Lijuan Song⁹, and Harald Kunstmann^{4,10,11} 

Key Points:

- The human-induced alterations of streamflow, extreme floods, and lake water level and storage are comprehensively analyzed
- A dynamic irrigation module for distinct crops is developed and coupled to reservoir operation with a cost-function-based approach
- A conceptual reservoir operation scheme is extended to include both water storage anomalies and water demand anomalies in hydrologic models

Supporting Information:

Supporting Information may be found in the online version of this article.

Correspondence to:

N. Dong,
dongnp@iwhr.com

Citation:

Hao, H., Dong, N., Yang, M., Wei, J., Zhang, X., Xu, S., et al. (2024). The changing hydrology of an irrigated and dammed Yangtze River: Streamflow, extremes, and lake hydrodynamics. *Water Resources Research*, 60, e2024WR037841. <https://doi.org/10.1029/2024WR037841>

Received 30 APR 2024
Accepted 11 SEP 2024

¹State Key Laboratory of Hydraulic Engineering Intelligent Construction and Operation, Tianjin University, Tianjin, China, ²State Key Laboratory of Simulation and Regulation of Water Cycle in River Basin, China Institute of Water Resources and Hydropower Research, Beijing, China, ³State Key Laboratory of Hydrology-Water Resources and Hydraulic Engineering, Hohai University, Nanjing, China, ⁴Institute of Meteorology and Climate Research (IMK-IFU), Karlsruhe Institute of Technology, Garmisch-Partenkirchen, Germany, ⁵Hydrology, Agriculture and Land Observation (HALO) Laboratory, Division of Biological and Environmental Science and Engineering, King Abdullah University of Science and Technology, Thuwal, Saudi Arabia, ⁶Key Laboratory of Water Cycle and Related Land Surface Processes, Institute of Geographic Sciences and Natural Resources Research, Chinese Academy of Sciences, Beijing, China, ⁷School of Civil and Hydraulic Engineering, Huazhong University of Science and Technology, Wuhan, China, ⁸Institute of Hydraulics and Ocean Engineering, Ningbo University, Ningbo, China, ⁹School of Geospatial Engineering and Science, Sun Yat-sen University, and Southern Marine Science and Engineering Guangdong Laboratory (Zhuhai), Zhuhai, China, ¹⁰Institute of Geography, University of Augsburg, Augsburg, Germany, ¹¹Centre for Climate Resilience, University of Augsburg, Augsburg, Germany

Abstract Understanding the role of anthropogenic activities in the hydrological cycle is critical to support sustainable water management for the Yangtze River Basin (YRB), which experiences extensive dam operation, irrigation and water withdrawal. However, this remains challenging due to insufficient accuracies of existing process-based models for fully depicting anthropogenic activities as part of the hydrological cycle. To this end, this study enhances a national-scale coupled land surface-hydrologic-hydrodynamic model (CLHMS) with a dynamic irrigation scheme for distinct crops, an extended reservoir operation scheme incorporating both water storage anomalies and water demand anomalies, and a cost-function-based approach to link water demands with reservoir operation. The enhanced model is extensively validated against historical streamflow, water storage of 90 reservoirs, and irrigation water withdrawal in the YRB, and the water level and storage of the Poyang Lake (PYL). By setting up controlled experiments in the YRB, we show that the streamflow decreases by 2%–6% due to irrigation and water withdrawal, and manifests an attenuated seasonality due to reservoir operation. At the basin scale, the increasing trend of extreme flood peaks exhibits a reversal under human activities, with the flood mitigation effect of irrigation and water withdrawal accounting for up to 50% of that of reservoir operation. The hydrodynamics of the PYL also exhibits considerable human-induced alterations, with a 1.79 m-decrease in the water level at the end of flood season. Our study sheds light on quantifying anthropogenic hydrologic impacts at basin scales, with important implications for understanding the co-evolution between anthropogenic activities and the hydrological cycle.

1. Introduction

Reservoir operation, irrigation and water withdrawal are main components of anthropogenic activities that play a major role in the natural-social dualistic water cycle (Abbott et al., 2019; Kåresdotter et al., 2022; Qin et al., 2014). Although global reservoirs have a significantly less total capacity compared to natural lakes, they constitute one of the most intensive human-induced modifications of the hydrological cycle (Chao et al., 2008; Li et al., 2023). This modification includes alterations of river flows (Garcia et al., 2020) and impacts on the water level, storage, and ecosystem of lakes within coupled river-lake systems (Liang et al., 2021; Zhang et al., 2022). Most reservoirs are designed with objectives including hydropower and flood control (Brunner, 2021; Zhang, Liu, et al., 2019; Zhang, Wang, & Niu, 2019), and they also serve as vital water sources for irrigation uses (Gonzalez et al., 2020; Zeng et al., 2017). As reservoirs increasingly support irrigation water supplies, irrigation has evolved into a critical component of the water cycle (Lo & Famiglietti, 2013; Wang et al., 2023). Globally, approximately

© 2024. The Author(s).

This is an open access article under the terms of the [Creative Commons Attribution-NonCommercial-NoDerivs License](https://creativecommons.org/licenses/by/4.0/), which permits use and distribution in any medium, provided the original work is properly cited, the use is non-commercial and no modifications or adaptations are made.

70% of freshwater withdrawals per capita are used for irrigation purposes (Chen, Han, et al., 2018; Chen, Niu, et al., 2018). In addition to agricultural irrigation, industrial and domestic water uses also consume substantial freshwater resources (Flörke et al., 2013). Overall, reservoir operation, irrigation and water withdrawal are considered to have exerted remarkable effects on the global water cycle.

To quantify the impacts of human activities on the water cycle, two approaches are widely used. The first involves employing long-term streamflow data to analyze the impacts of human activities on the water cycle before and after a specific time point (Gao et al., 2011; Guo et al., 2012; Zhang et al., 2022). However, this method struggles to differentiate the effects of human activities from those of climate change and is particularly challenged in quantifying the relative impacts of various components of human activities. Consequently, hydrological modeling is increasingly gaining attention for understanding the hydrologic alterations under multiple drivers (Gou et al., 2021; Lin et al., 2019), especially human impacts. Several state-of-the-art global hydrological models have explicitly included mechanisms for reservoir operation, surface water, and groundwater processes (Pokhrel et al., 2021; Zajac et al., 2017), and have exhibited satisfactory performance in simulating observed streamflow in many regions across the globe (Hanasaki et al., 2018; Müller Schmied et al., 2021; Sutanudjaja et al., 2018; Wada et al., 2016). Additionally, irrigation and human water withdrawals are increasingly represented in large-scale hydrological models (Abeshu et al., 2023; Alcamo et al., 2003; Chen, Han, et al., 2018; Chen, Niu, et al., 2018; Döll et al., 2012; Haddeland et al., 2006; Wada et al., 2011), and land surface models (Leng et al., 2014; Nie et al., 2018; Pokhrel et al., 2012).

While above studies have substantially enhanced our understanding of the hydrologic impacts of human activities, challenges remain at basin scales. Although global hydrological models have been extensively validated and highly valuable at larger scales, they often exhibit relatively less accuracies at more localized levels due to the complexity of human activities across different regions (Beck et al., 2017). This underscores the need for further improvements in representing human activities, especially reservoir operation and irrigation practices. Traditional hydrological models typically use two types of reservoir operation schemes: the first type, demand-driven schemes, primarily consider downstream water demands as the main control for reservoir releases, with reservoir storage conditions playing a minor role, if any (Voisin et al., 2013; Wisser et al., 2010); the second type, target storage-based schemes, relate the reservoir releases to the reservoir water storages at different times of the year (Dong et al., 2022, 2023; Yassin et al., 2019). However, in practice, reservoir operators often consider both the water storage and the water demand when determining the reservoir releases. Yet, current schemes that balance water availability and demands are not fully developed. This gap may be due to challenges in accurately simulating irrigation water demands and coupling them with reservoir operation. For example, many recent irrigation schemes overlook paddy irrigation, which requires the depiction of a flooded pond, potentially leading to an underestimation of water demands (Leng et al., 2017; Xu et al., 2019). In addition, large-scale hydrologic models typically link irrigation water demand to reservoirs based merely on horizontal distance (Hanasaki et al., 2006), which neglects the factors of vertical distance and water availability. These issues add to the hydrological modeling uncertainties under human impacts (Yin et al., 2021).

These difficulties in accurately parameterizing human activities, combined with the lack of localized calibration of large-scale hydrological models, pose a challenge in accurately identifying the human-induced hydrological variations. This is particularly the case for the Yangtze River Basin (YRB), which is home to one of the largest groups of mega-reservoirs globally. Irrigation and other water withdrawals of the basin exceed 200 billion m³ per year, accounting for 30% of the national total water use. With these increasing human activities, its impact on extreme floods and the wetland ecosystem is of growing concern. For instance, in terms of extreme floods, the third largest flood over the past 100 years occurred in 2020, with the Three Gorges Reservoir experiencing an inflow peak of 78,000 m³/s (Wang, Peng, et al., 2021; Wang, Yang, et al., 2021). Besides, the YRB contains China's largest freshwater lake, the Poyang Lake (PYL), which has an annual maximum area of around 4,000 km². The variation of lake water level and storage has a profound impact on the hydro-ecological system (Li et al., 2022; Liu et al., 2020; Mu et al., 2022). Therefore, accurately identifying the variation of streamflow, extreme floods, and lake hydrodynamics under human impacts is crucial for sustainable water resource management and ecological conservation.

To this end, we develop a dynamic irrigation scheme for distinct crops, an extended reservoir operation scheme incorporating both water storage anomalies and water demand anomalies, and a cost-function-based approach to link water demands with reservoir operation, which are then fully integrated into the national-scale coupled land

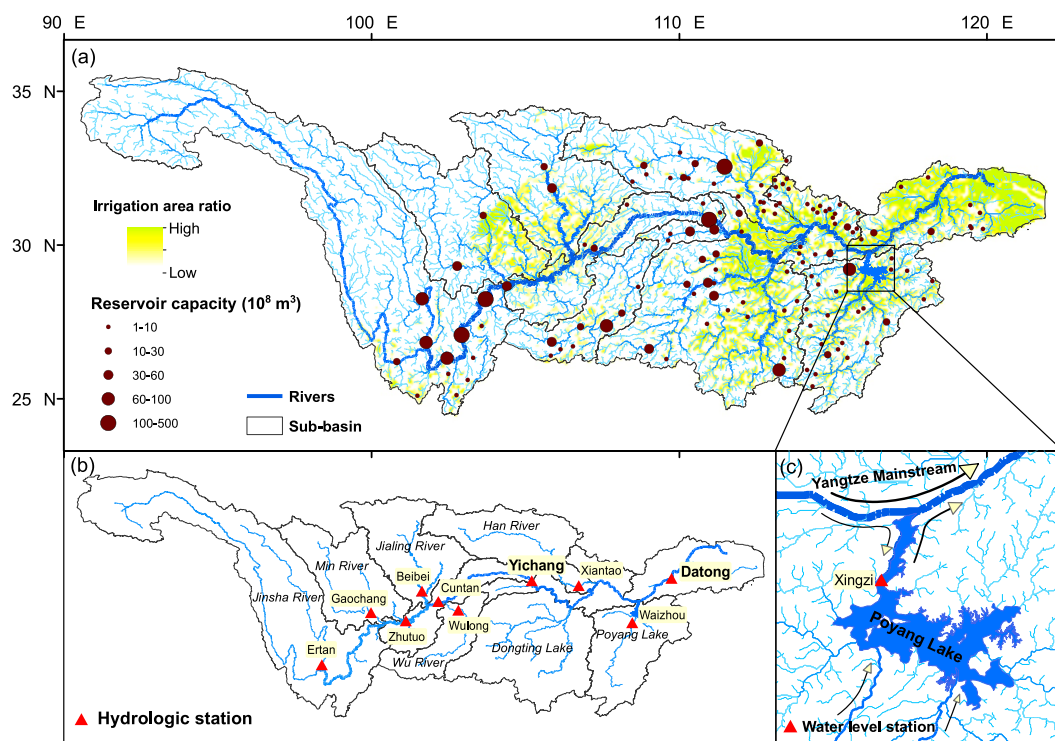


Figure 1. (a) Irrigated areas and 133 large reservoirs and (b) hydrologic stations in the Yangtze River Basin, and (c) the river-lake system of the Yangtze mainstream and the Poyang Lake, where the river-lake flow is bidirectional. Arrows represent the flow directions.

surface-hydrologic-hydrodynamic model (CLHMS). By applying the model to the YRB, we aim to address the following scientific question: To what extent have human activities, especially large-scale reservoir operation and irrigation, altered the streamflow, extreme floods, and the hydrodynamic processes of the Poyang Lake in the YRB? This study is expected to provide implications for water resources management, particularly in addressing climate change and promoting ecological balance in the basin.

2. Study Area and Data

2.1. Study Area

The Yangtze River is the third longest river in the world, and drains an area of 1.8 million km², accounting for about 20% of China's total land area (Gong et al., 2006). The average annual precipitation and annual streamflow are approximately 1,100 mm and 28,000 m³/s, respectively. Precipitation and streamflow in the basin exhibit strong seasonality, with 76% of the annual precipitation occurring from April to September (Zhang, Chao, et al., 2015). The basin is home to China's largest freshwater lake, the PYL, which receives inflow from its catchment (the Poyang Lake Basin) and then discharges northward into the mainstream of the Yangtze River. There is a mutual backwater effect between the lake and the mainstream of the Yangtze River (Wang, Peng, et al., 2021; Wang, Yang, et al., 2021; Xu et al., 2020; Zhang, Chen, et al., 2015), with the river water flowing back into the lake when the water level of the Yangtze mainstream is higher than the lake water level, and vice versa (Figure 1c).

There are 10 major hydrological stations across the basin, including Pingshan, Gaochang, Zhutuo, Beibei, Cuntan, Wulong, Yichang, Xiantao, Waizhou, and Datong (Figure 1b). Among these, Pingshan, Gaochang, and Beibei are the control stations for the Jinsha River Basin, Min River Basin, and Jialing River Basin, respectively; Wulong, Xiantao, and Waizhou are the control stations for the Wu River Basin, Han River Basin, and the PYL basin. Yichang is the control station for the upper YRB and is also the downstream hydrological station for the Three Gorges Dam (TGD). Datong is the outlet control station for the entire YRB.

The YRB is a major economic, agricultural, and industrial hub of China, currently supporting about one-third of the population and gross domestic product of the country. Over the past 30 years, a significant number of reservoirs have been constructed in the basin, with the total storage capacity increasing from less than 100 billion m³ in 1991 to about 360 billion m³ in 2022. There are approximately 133 large reservoirs with a strong impact on the monthly streamflow in the YRB (Figure 1a), with a total storage capacity of 234 billion m³ or approximately two-thirds of the total storage capacity of the basin. In addition, the YRB accounts for the highest water consumption of approximately 90 billion m³ across the country, and more than 70% is used for irrigation. Irrigation in the YRB is primarily concentrated in the Min River Basin, Jialing River Basin, and the downstream Dongting Lake Basin, Han River Basin, and PYL basin (Figure 1a). In recent years, the irrigated area in the YRB has continuously expanded and increased by over 5,000 thousand hectares during 1991–2022, with a corresponding increase in the irrigation water withdrawal.

2.2. Data

Streamflow data. To validate the streamflow simulations, we collected monthly streamflow data from 1991 to 2020 for 10 hydrological stations in the YRB, and daily streamflow data of the Yichang and Datong stations for the period from 2011 to 2022.

Reservoir data. To achieve the reservoir operation simulations, we gathered basic information on 133 large reservoirs in the YRB, including their capacities and locations. These reservoirs are designed with multiple objectives and have a storage capacity ranging from 0.1 to 45.07 km³ (see Table S1 in Supporting Information S1). Additionally, the in-situ daily inflow, release, and water storage of 90 reservoirs were collected to calibrate and validate the reservoir operation simulations.

Irrigation area and crop data. To depict the spatial distribution of crop areas and their growth stages, we collected the Global data set of Monthly Irrigated and Rainfed Crop Areas (MIRCA-OS) (Kebede et al., 2024), which is an updated version of the MIRCA2000 (Portmann et al., 2010). This data set includes irrigation area of 23 crops, including single-cropping rice and double-cropping rice, at a 5 arc-minute grid resolution for the years 2000, 2005, 2010, and 2015 in a consistent manner. Before use, the irrigation area is corrected with a scaling factor based on provincial statistics spanning from 1991 to 2022.

Irrigation water data. To validate the modeled irrigation water demand in our simulations, we collected the annual irrigation water withdrawal statistics for each sub-basin within the YRB published by local water authorities from 2004 to 2022.

Lake water level and storage data. To validate hydrodynamic simulations of the PYL, we collected monthly water level data of the Xingzi station for the years 2010–2020. Additionally, we gathered the monthly water storage variations of the PYL from 2017 to 2020, which is derived from Sentinel-1 SAR data and cloud-free Sentinel-2 images combined with lake bathymetry (Song et al., 2021). We consider this data as the reference water storage for comparison with our storage simulations.

3. Methods

3.1. National-Scale Coupled Land Surface-Hydrologic-Hydrodynamic Model CLHMS

We employ the CLHMS model to analyze the human-induced alterations of the streamflow, extreme floods, and hydrodynamics of the PYL in the YRB. The CLHMS (version 2.0) is a national-scale, fully coupled modeling system of the land surface scheme of LSX and the physically-based distributed hydrological model of Hydrologic Model System (HMS) for China (Dong et al., 2022). Note that the HMS here is different from the HEC-HMS model developed by the U.S. Army Corps of Engineers. The LSX consists primarily of a six-layer soil scheme, a two-layer vegetation scheme, a two-layer snow scheme and a glacier/icesheet scheme, and is capable of solving the water and energy balance in the snow-vegetation-soil continuum and on the glacier areas (Yu et al., 1999, 2006). The HMS derives the surface runoff routing with the diffusion wave equation, and is fully coupled with a 2-D groundwater routing model, which allows the model to compute the groundwater dynamics on a raster grid basis (Wagner et al., 2016). In particular, the HMS is extended to explicitly simulate the area and storage dynamics of floodplains and natural lakes by solving the two-dimensional diffusion wave equations in the river-lake-floodplain continuum:

$$\frac{dV_l}{dt} = \frac{d}{dx} \left[A \frac{m}{r} D^{2/3} \left| \frac{dh_l}{dx} \right|^{-1/2} \left(\frac{dh_l}{dx} \right) \right] + \frac{d}{dy} \left[A \frac{m}{r} D^{2/3} \left| \frac{dh_l}{dy} \right|^{-1/2} \left(\frac{dh_l}{dy} \right) \right] + (1 - f_w)R + f_w(P - E - C_u - C_g) - C_l \quad (1)$$

where V_l represents the average depth of surface water; A is the cross-sectional area of the river or lake at the grid boundary; r is the roughness; D is the depth of the river or lake; R is the surface runoff; $P - E$ represents the net precipitation minus evaporation over the water body; f_w is the surface water area ratio; the Manning water flow terms are calculated for the eight directions between grids.

The model has been well calibrated against the natural streamflow for 1961–1980 in our previous study, see Dong et al. (2022) for the driving data and relevant details.

3.2. A Dynamic Irrigation Scheme for Distinct Crops

To achieve the simulation of irrigation water demands, we develop an irrigation scheme that is suitable for distinct crops, which is then fully coupled to the CLHMS model. The global data set MIRCA-OS, an updated version of the widely used MIRCA2000 data set, is employed to obtain specific planting calendars and growth season lengths for various crops (Kebede et al., 2024). A total of 23 crop species are considered, which we mainly categorize as paddy and non-paddy crops that are separately parameterized in the model.

For paddy crops, in light of the need to maintain a certain water depth during the rice growth stages, this study employs the water balance method for paddy fields to estimate irrigation water demand. It is assumed that irrigation is applied whenever the water depth in the paddy fields falls below 50 mm, until 2 weeks before harvest (Wisser et al., 2008, 2010). The irrigation water demand for paddy crops, IWR_p , and the water balance equation for paddy fields are as follows:

$$IWR_p = \max(0, S_{max} - (S_{t-1} + P_t)) \quad (2)$$

$$S_t = S_{t-1} + P_t + IWR_p - E_t - I_t \quad (3)$$

where S_{max} indicates the water depth necessary to sustain rice growth, assumed as 50 mm; S_{t-1} represents the surface water depth at the previous timestep; S_t represents the surface water depth at the current timestep; P_t is precipitation; E_t represents the water evaporation calculated with the Penman formula; I_t indicates the infiltration from the surface water layer to the first soil layer.

During rice cultivation, farmers first carry out land preparation through tilling and compaction to ensure a low permeability of the soil. This practice ensures the paddy roots can remain submerged (Devanand et al., 2019; Janssen et al., 2010; Joseph & Ghosh, 2023). In the CLHMS model, we represent the reduced infiltration caused by soil compaction with a coefficient f_p ranging from 0 to 1:

$$I_t = f_p \cdot I_{max} \quad (4)$$

where I_{max} represents the maximum infiltration rate, which is assumed to be the saturated hydraulic conductivity; f_p varies in different models, typically between 0.001 and 0.1 (Joseph & Ghosh, 2023; Wada et al., 2014). In this study, we calibrate the parameter to be a uniform value of 0.004 across the basin.

For each of the non-paddy crops, we calculate its irrigation water demand following the Global Crop Water Model (GCWM, Siebert & Doell, 2008). An advantage of this model is its ability to distinguish between the growth characteristics and corresponding water requirements of each non-paddy crop. The irrigation water demand, IWR_{np} , can be calculated as:

$$IWR_{np} = (1 - k_s) \cdot k_c \cdot ET_0 \quad (5)$$

where k_c is the crop coefficient that varies across crops at a daily basis. The crop coefficient is calculated from the crop coefficient curve, derived at the daily scale for each crop during its entire growth period (Allen et al., 1998;

Xia et al., 2022); ET_0 is the reference evapotranspiration; k_s is a dimensionless reduction coefficient to calculate the actual evapotranspiration under water stress:

$$k_s = \begin{cases} \frac{S}{(1-p)S_{max}} & S < (1-p) \cdot S_{max} \\ 1 & S \geq (1-p) \cdot S_{max} \end{cases} \quad (6)$$

$$p = p_{std} + 0.04 \cdot (5 - k_c \cdot ET_0) \quad (7)$$

where S represents the actual available soil water content; S_{max} is the total available soil water capacity; p is the proportion of S_{max} that a crop can extract from the root zone without suffering from water stress, which depends on the crop type and the maximum crop evapotranspiration; p_{std} is the specific depletion fraction of each crop.

The total irrigation water demand, IWR , is therefore the sum of irrigation water demands for paddy IWR_p and for non-paddy crops IWR_{np} . In addition to irrigation water, the model considers industrial and domestic water use, see Dong et al. (2022) for details.

3.3. An Extended Reservoir Operation Scheme With Water Storage/Demand Anomalies

The D22 conceptual reservoir operation scheme, developed in our previous studies, is used to simulate the reservoir operation in the CLHMS. D22 has two slightly different versions: one for reservoirs with historic inflow, release, and storage data available for calibration (Dong et al., 2023), and another for reservoirs lacking such data (Dong et al., 2022). For the 90 reservoirs with historic operation data in this study, the reservoir release, Q_t , is calculated with the former version of the D22 based on the current water level relative to several reservoir pool storages:

$$Q_t = \begin{cases} \min\left(Q_{min}, \frac{V_t}{\Delta t}\right) & (V_t \leq V_d) \\ \max(Q_{min}, r_t \cdot Q_{tar}) & (V_d < V_t \leq V_c) \\ r_t \cdot Q_{tar} + (Q_s - r_t \cdot Q_{tar}) \cdot \left(\frac{V_t - V_c}{V_f - V_c}\right)^k & (V_c < V_t \leq V_f) \\ \max\left(Q_s, \frac{V_t - V_f}{\Delta t}\right) & (V_t > V_f) \end{cases} \quad (8)$$

where V_p , V_d , V_c and V_f are the water storages of reservoirs at the model time step t , at the dead storage level, conservation level, and high flood level, respectively; Q_{min} is the minimum release; Q_s is the maximum acceptable release; k ($k \leq 1$) is a flood indicator equal to the ratio of Q_s to the inflow; Q_{tar} is the daily target releases that implicitly represent the multi-year averaged water demands at the different times of the year, calculated as the 10-day moving average of the multi-year median (mean) of daily releases for within-year (over-year) reservoirs (Dong et al., 2023).

In the original D22 scheme of Equation 8, r_t is a parameter to reflect the impact of water storage anomalies (i.e., the relative difference between the current storage V_t and the target storage V_{tar}) on the reservoir release:

$$r_t = 1 + c \cdot \frac{V_t - V_{tar}}{V_{cd} - V_d} \quad (9)$$

where V_{tar} is the daily target storage, calculated as the 10-day moving average of the multi-year median (mean) of daily storages for within-year (over-year) reservoirs; and c is a calibrated parameter. The rationale behind r_t in the original scheme is to adapt the release only to the storage anomalies relative to the target storage, with the assumption that the socio-economic water demands of reservoirs can be represented by the target releases that do not change over different years. However, water demands (especially for irrigation) often fluctuate across years, and the water demand anomalies can also be a consideration when dam operators determine the release.

Therefore, in this study, we extend Equation 9 of the original scheme by introducing the water demand anomalies (i.e., the relative difference between the current water demand W_t and the target water demand W_{tar}) in the expression of r_t :

$$r_t = 1 + c \cdot \frac{V_t - V_{tar}}{V_{cd} - V_d} + f \cdot \frac{W_t - W_{tar}}{W_{max} - W_{min}} \quad (10)$$

where the terms $\frac{V_t - V_{tar}}{V_{cd} - V_d}$ and $\frac{W_t - W_{tar}}{W_{max} - W_{min}}$ denote the water storage anomalies and the water demand anomalies, respectively; f is a calibrated parameter which, together with c , serves as the weight of release decision preferences. Here, the water demand includes industrial, domestic, hydropower, and irrigation water demand. According to the monthly electricity generation data (IEA, 2024) and the monthly industrial, irrigation, and domestic water withdrawal data (Huang, Hejazi, et al., 2018; Huang, Long, et al., 2018) over recent years, the monthly variability of industrial, domestic, and hydropower water demands across years is minor compared to that of irrigation. Therefore, the water demand anomalies are simplified as the irrigation water demand anomalies in this study, and W_t , W_{tar} , W_{max} and W_{min} represent the irrigation water demand of a reservoir at the date t , its multiyear average for that day, and the multiyear average daily maximum and minimum values, respectively. They are all computed as the moving average of the sum of water demands linked to that reservoir for the previous 30 days. Take W_t for example:

$$W_t = \sum_{(i,j) \in A} \sum_{k=1}^{30} \frac{IWR_{t-k+1}(i, j)}{30} \quad (11)$$

where $IWR(i, j)$ is the simulated irrigation water demand at the grid point (i, j) (Section 3.2); and A represents all irrigation water demand grid points linked to the reservoir, and is determined with a cost-function-based approach described as follows.

In the cost-function-based approach, irrigation water demands are assumed linked to a reservoir if they abstract water from a river section controlled by that reservoir. Here, a river section is considered controlled by a reservoir if the reservoir controls over half of its average streamflow, until it reaches the next downstream reservoir. To link irrigation demand to its abstraction point and hence its controlling reservoir, we introduce a generalized cost function that implicitly represents the economic costs of transferring water from the abstraction point to the demand location, following Zhou et al. (2021), that is,

$$C = \frac{D^{\text{path}} + k \cdot H^{\text{path}}}{\log(U + 1)} \quad (12)$$

where C is the cost along the water transfer path; D^{path} and H^{path} represent the horizontal and vertical distances along the path, respectively; k is a factor that reflects the higher difficulty (and cost) of lifting water vertically compared to transferring it horizontally, set to 10,000 following Zhou et al. (2021); U accounts for water availability, represented by the average simulated streamflow at the abstraction point. To account for the impact of elevated water height due to reservoir impoundment on the vertical distance, H^{path} is calculated as:

$$H^{\text{path}} = \max(0, \alpha - 30 \cdot \beta) \quad (13)$$

where α is the cumulative elevation increments along the path; β is a binary value that equals to 1 if a dam is present in the abstraction grid cell, and 0 otherwise. β is multiplied by 30 m, which is the average height by which reservoir impoundment raises the water level from dead level to conservation level in the YRB.

By minimizing the cost function to locate the abstraction point for each water demand grid cell, we can identify all irrigation water demand grid cells that abstract water from river sections controlled by a reservoir (i.e., A in Equation 11). This approach offers an alternative for coupling water demands with reservoir operations in large-scale modeling studies, which typically link water demand to its abstraction point based solely on horizontal distance.

To implement the reservoir operation simulations, the four parameters, Q_{min} , Q_s , c and f , are calibrated for the 90 reservoirs with historic operation data. For the remaining 43 reservoirs that lack operation data, we use the D22 version designed for data-scarce reservoirs, as detailed in our previous research (Dong et al., 2022).

3.4. Experimental Design

To quantify the impact of various human activities on the streamflow, extreme floods, and lake hydrodynamics, three controlled simulation experiments are designed, namely a natural scenario (NAT) without consideration of human activities, a reservoir scenario (RES) considering only reservoir operation, and a human activity scenario (HUM) considering reservoir operation, irrigation and water withdrawal. All of these simulations are performed from 1991 to 2022. We quantify the human impacts by comparing the simulation results under these scenarios. In terms of streamflow, the human impact is quantified as a percentage of the natural streamflow (i.e., relative change of streamflow), which can provide a clear picture of how human interventions alter the water balance relative to natural flow conditions (Álamos et al., 2024; Dang & Pokhrel, 2024; Dariane & Pouryafar, 2021; Liu et al., 2019).

In all three experiment simulations (NAT, RES, and HUM), the model runs on a 5-km raster grid basis with daily resolution. Based on these simulations, the impact of anthropogenic activities on streamflow is analyzed monthly for 10 major hydrologic stations in the YRB. The effect on extreme floods is assessed daily for the mainstream Yichang and Datong stations. The impact on the water level at Xingzi station and the water storage of Poyang Lake is analyzed monthly.

4. Results

4.1. Model Evaluation Against Streamflow Observations

Model simulations under NAT and HUM are performed to evaluate the model performance in reconstructing the streamflow under human impacts across the YRB. Figure 2 depicts the streamflow simulations of 10 hydrologic stations for 1991–2022. For the period of 1991–2000, the Nash-Sutcliffe Efficiency (NSE) for NAT simulations at the mainstream stations of Pingshan, Zhutuo, and Cuntan ranges from 0.85 to 0.94; for Gaochang, Beibei, and Wulong at upstream tributaries, the NSE ranges from 0.87 to 0.90; for Waizhou at the PYL basin, the NSE is 0.94; and for the Xiantao station at the Han River Basin, the NSE is -1.27 , likely due to the operation of the Danjiangkou Reservoir completed in 1973. Notably, the Yichang station and the Datong station record NSE values of 0.96 and 0.98 under NAT, respectively. Overall, the model is able to well simulate the streamflow of the YRB in 1990s.

With the increasing human activities, the NSE values under NAT show a decreasing trend from 1991 to 2022 at all hydrological stations. During 2013–2022, for example, Yichang drops from 0.87 to 0.60, and Datong from 0.92 to 0.85 (Figure 2). By incorporating reservoir operation, irrigation and water withdrawal into the model, the simulation accuracy is significantly improved. In particular, the NSE of Yichang increases from 0.60 to 0.91, and Datong from 0.85 to 0.96. This indicates that the enhanced model is able to accurately capture the flow dynamics of the YRB under human activities.

To further validate the model in simulating daily streamflow and extreme floods, Yichang and Datong that control the upper YRB and the entire YRB are selected for analysis, respectively (Figure 3). The NSE of the simulated daily streamflow at Yichang for 2015–2022 improves from 0.43 to 0.82 by coupling reservoirs, irrigation and water withdrawal, and daily simulations at Datong sees an improved NSE from 0.83 under NAT to 0.94 under HUM for 2011–2020. Similarly, the simulated annual maximum flood peaks show a great improvement by considering human activities, with R^2 values increasing from -3.62 to 0.79 for Yichang, and from 0.65 to 0.86 for Datong, respectively. For example, the average observed annual maximum flood peak at Yichang is 37,786 m^3/s , while the average simulated flood peak under NAT (HUM) is 46,812 (37,420) m^3/s , with a relative error of 24.9% (-0.9%). This indicates that the enhanced model can well capture extreme floods under human activities.

4.2. Model Evaluation of Reservoir Operation Simulations

A total of 133 reservoirs are included in the model simulations. To evaluate the effectiveness of the cost-function-based approach in identifying the irrigation areas covered by each reservoir in the CLHMS model, we compare the simulated reservoir irrigation areas to their design irrigation areas. Design irrigation areas are difficult to

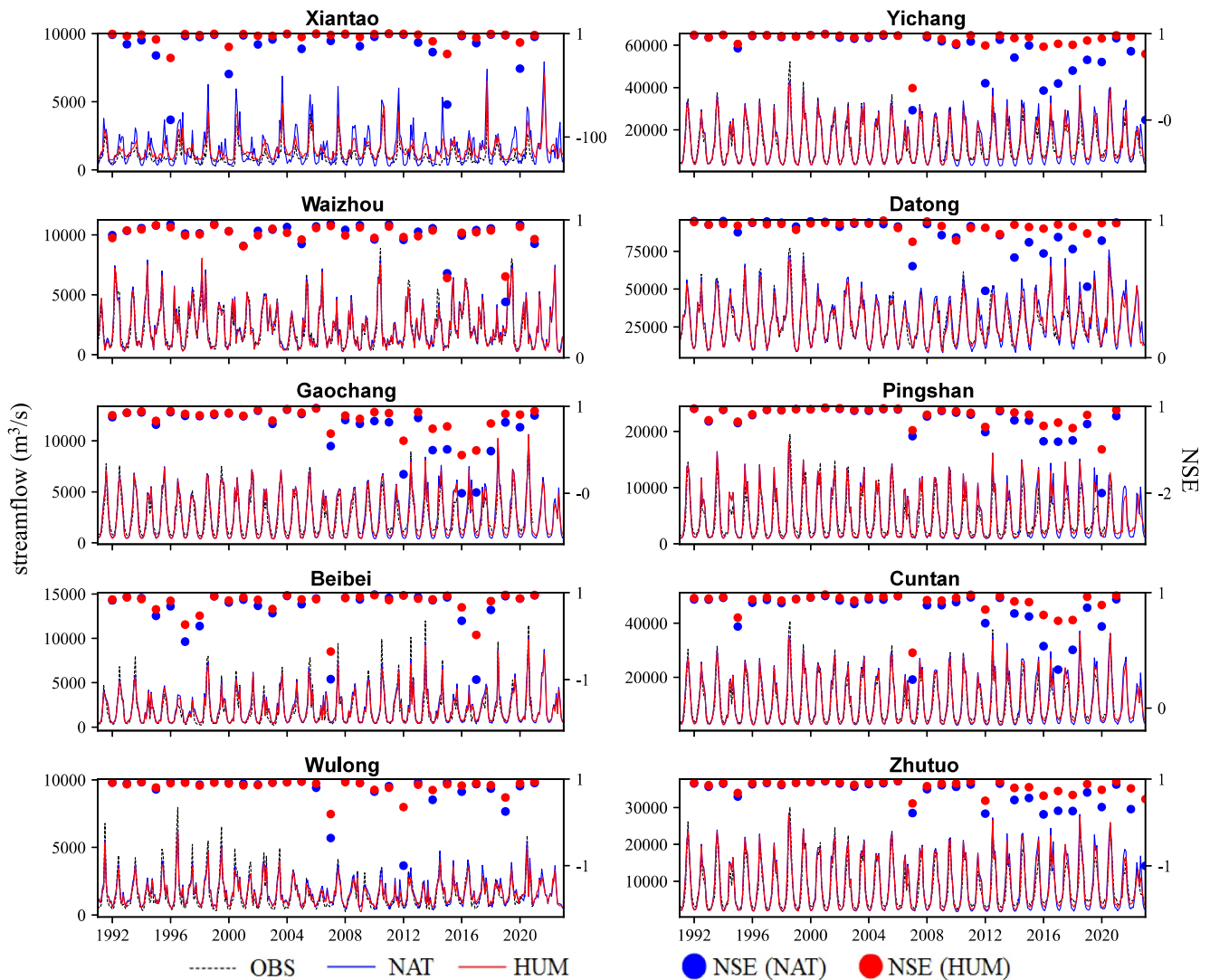


Figure 2. The observed monthly streamflow (OBS), the simulated natural streamflow (NAT), and the simulated streamflow considering human activities (HUM) at 10 hydrologic stations in the Yangtze River Basin. NSE: Nash-Sutcliffe Efficiency for each year.

obtain for most reservoirs; however, we managed to obtain the design irrigation areas for three reservoirs: Tingzikou, Xiangjiaba, and Chencun, from their reservoir design reports approved by water authorities. As shown in Figure 4, the simulated extent of irrigation areas for these three reservoirs generally matches well with their designs. This result indicates that the cost-function-based approach is effective for identifying irrigation areas of reservoirs in large-scale hydrologic models.

In terms of the reservoir operation simulations, the median NSE of simulated daily storages for the 90 reservoirs with operation data is 0.56, and the median correlation coefficient (R) is 0.79. Note that the reservoir operation simulations are driven by simulated inflow. Figure 5 shows the daily simulated storages for the 24 relatively large reservoirs, which account for 77% of the total capacity of the 133 reservoirs, and over 50% of that of all reservoirs in the YRB. The median NSE for these reservoirs is 0.67, and the median R is 0.85, with over 92% of the reservoirs with an R greater than 0.70, and approximately 88% with an NSE greater than 0.50. Among them, the TGD and the Danjiangkou Reservoir, China's two largest reservoirs, have an NSE of 0.94 and 0.81, and an R of 0.97 and 0.90, respectively.

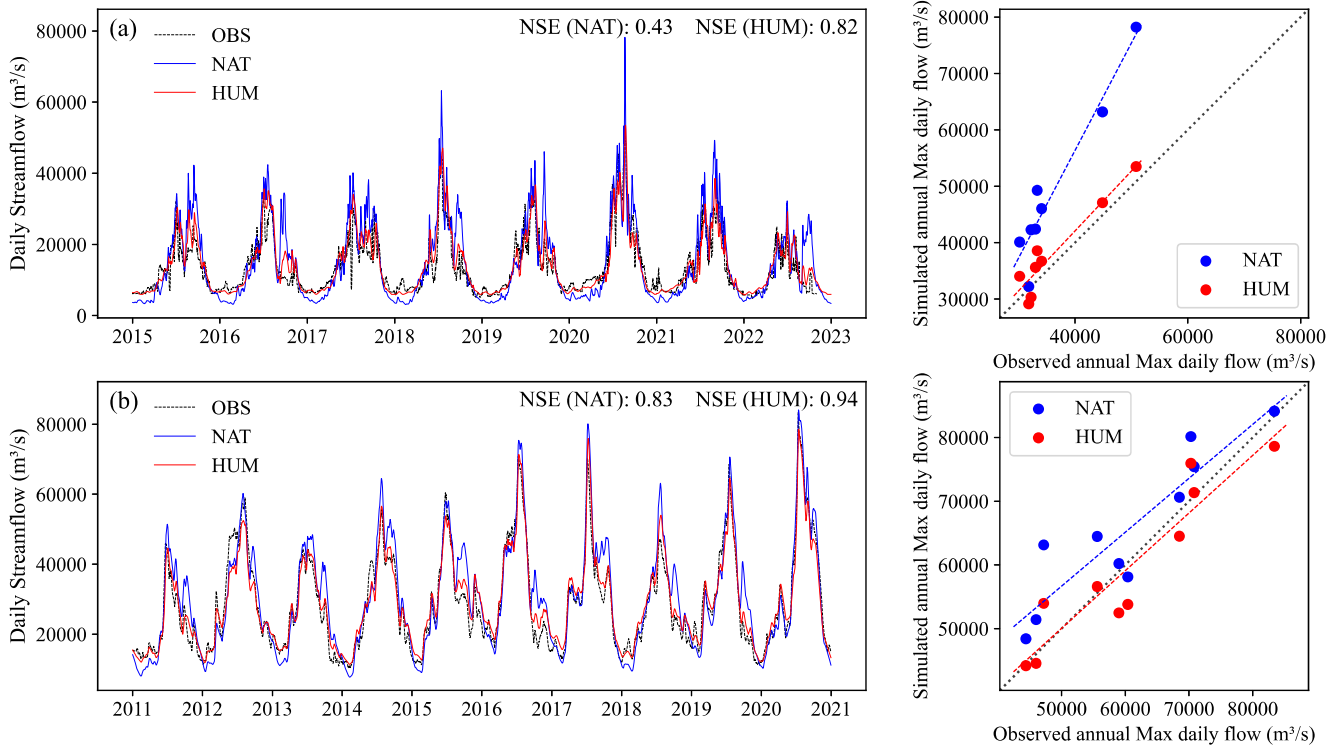


Figure 3. The observed and simulated daily streamflow (left) and annual maximum flood peaks (right) under NAT and HUM at (a) Yichang and (b) Datong in recent years.

The reservoirs simulated in our study serve varying purposes, including flood control, irrigation, and hydropower, with varying regulating abilities (annual, multi-year, seasonal). This result shows the enhanced model is generally able to well reconstruct the operation for a wide range of reservoirs in the YRB.

4.3. Model Evaluation Against Irrigation Water Statistics

Figure 6 shows the simulated annual irrigation demands compared with published statistics in the 11 subbasins for 2004–2022. The simulated irrigation demand shows good spatial consistency with the reported irrigation water

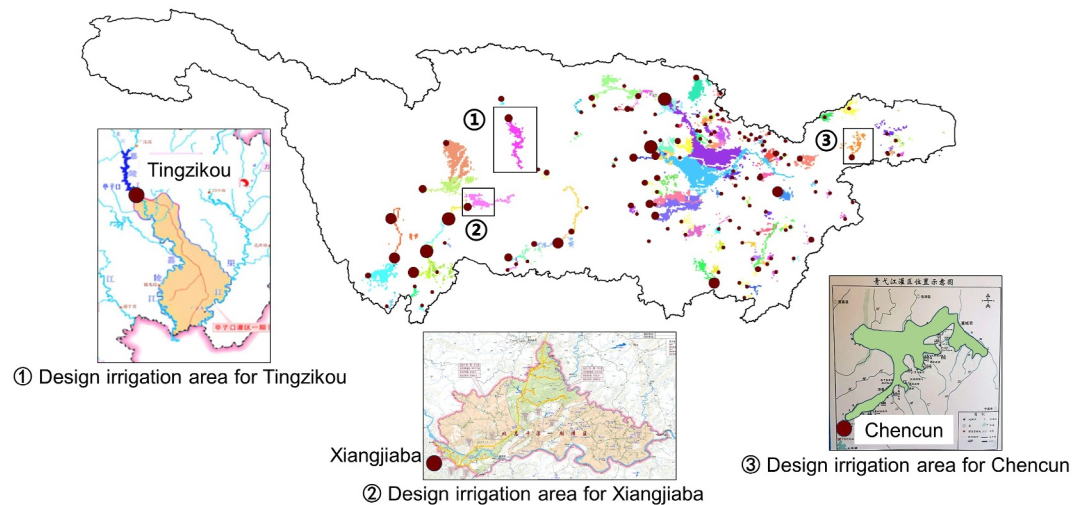


Figure 4. Simulated irrigation area of reservoirs shown in shaded areas with distinct colors for each reservoir, and the design irrigation area of Tingzikou, Xiangjiaba and Chencun Reservoirs in subplots for comparison.

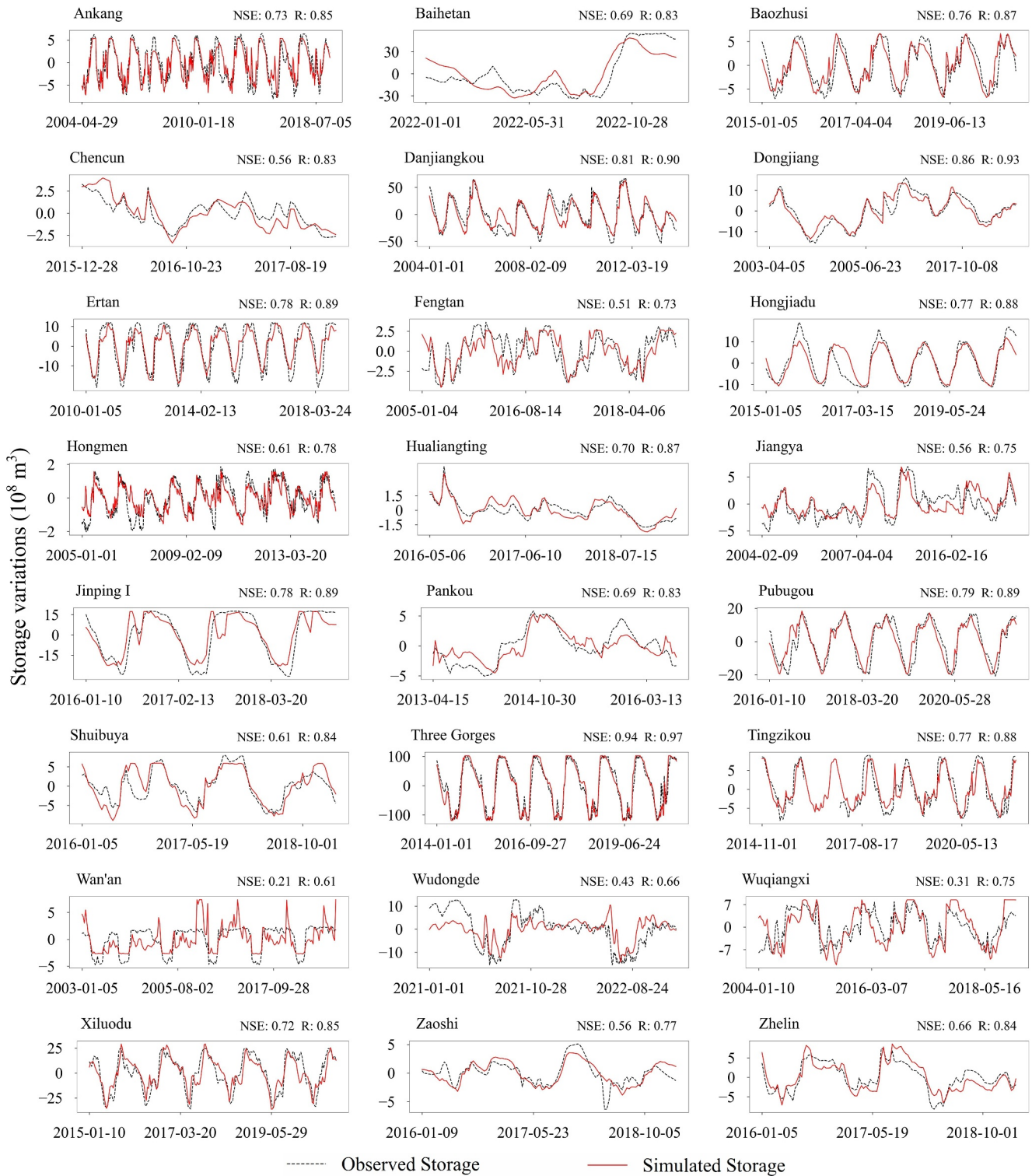


Figure 5. Simulated daily water storage variations of 24 largest reservoirs in the Yangtze River Basin under HUM, as compared with observations. The reservoir operation simulations are driven by simulated inflow and are carried out in an online mode within the CLHMS model.

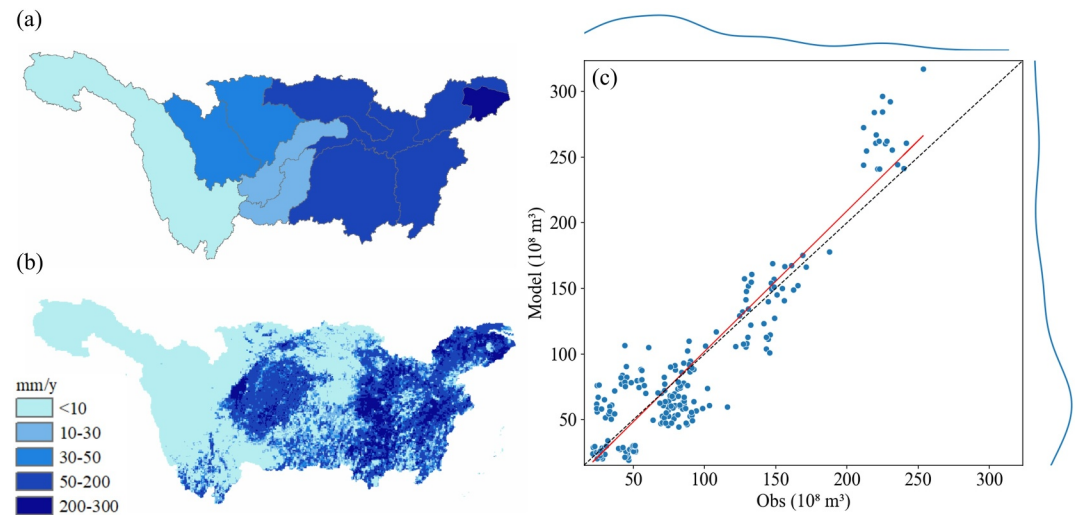


Figure 6. (a) The reported annual irrigation water demands in different subbasins of the Yangtze River Basin, (b) the simulated annual irrigation water demands, and (c) the scatterplot of simulated and reported irrigation water demands for 2004–2022 in different subbasins.

statistics. Yearly scatter plots (Figure 6c) indicate that the model can effectively reconstruct annual irrigation demands across different subbasins, with an R^2 of 0.80 and a relative error of 1%.

The average annual irrigation in the YRB is 57 mm, with the least in the Jinsha River Basin at 4.8 mm, which is characterized by rigid terrain and sparse population (Zhan et al., 2018), leading to lower irrigation water demands. The river delta shows the highest average annual irrigation demands of ~ 200 mm due to the plain terrain and its status as a major rice-producing area in China (Jiao et al., 2018). Further analysis (Figure 6b) reveals that areas with annual irrigation demands less than 10 mm cover 0.86 million km^2 (49% of the basin area), primarily located in the Jinsha, Wu, and upper Han River Basin. Demands between 10 and 50 mm span 0.32 million km^2 (17% of the basin area), primarily in the lower Jinsha Basin and the lower YRB. Areas with demands over 50 mm cover 0.62 million km^2 (34% of the basin area), mainly in basins of the Jialing River, Dongting Lake, lower Han River, PYL, and the lower mainstream.

4.4. Model Evaluation Against Lake Water Level and Storage Variations

To validate the simulation of the hydrodynamic processes of the PYL, the water level at Xingzi and the reference lake storage variations are analyzed. Note that the simulated water levels are normalized by removing the mean bias due to DEM imprecisions. The NSE of water level simulations from 2010 to 2020 at Xingzi is 0.81 (0.94), with an R of 0.93 (0.97) under NAT (HUM) (Figure 7a). The model underestimates the low water levels and overestimates high water levels under NAT, and performs much better with the inclusion of human activities. For 2017–2020, the simulated lake storage variations also match well with the reference data after considering human activities in the model, with the NSE increasing from 0.15 to 0.65 (see Figure S3 in Supporting Information S1).

In addition, the JRC global surface water data set is employed to depict the water occurrence in the PYL, which provides the rasterized monthly water extents at a global scale with a spatial resolution of approximately 30 m (JRC, 2016; Pekel et al., 2016). Figure 7b compares the GSW-based and model-simulated water occurrence for 1991–2020 under HUM, which shows that the model is generally able to well simulate the area dynamics of the PYL.

4.5. Human-Induced Streamflow Alterations

The human-induced streamflow alterations are quantified over three periods, namely 1991–2000, 2001–2012, and 2013–2022. Figure 8 illustrates the monthly streamflow and its alterations under human impacts for 2013–2022, with the results for the other two periods shown in the Supporting Information S1.

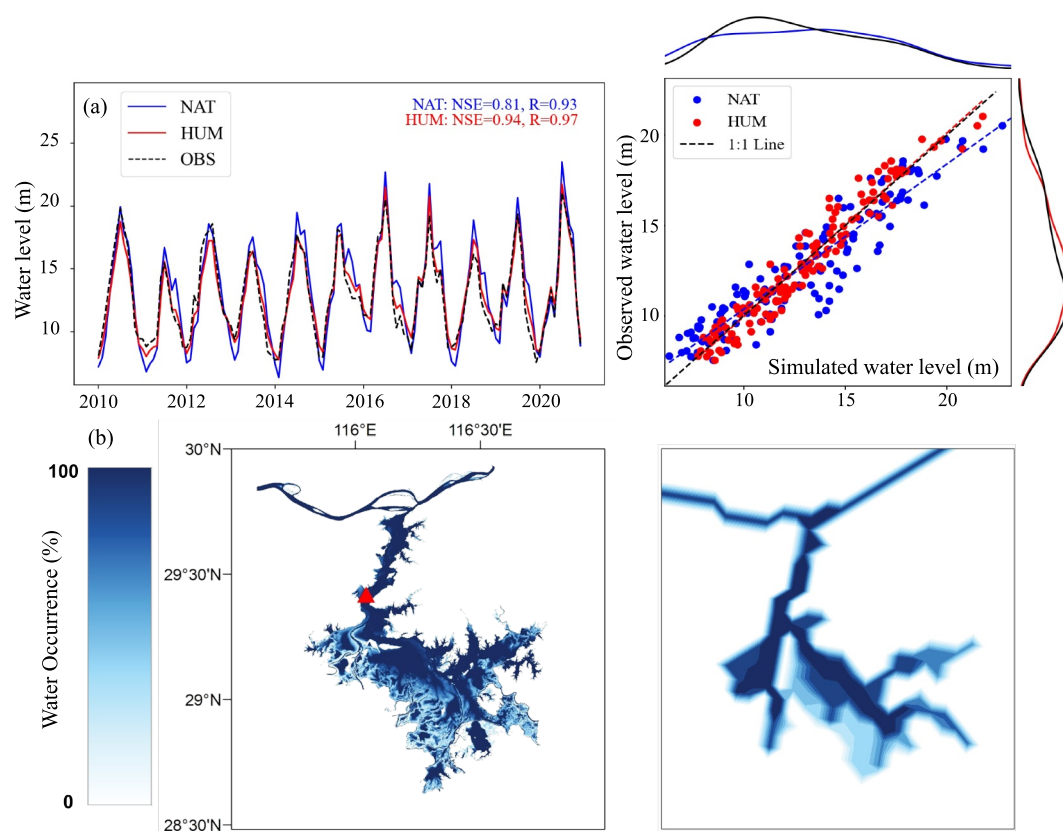


Figure 7. (a) The observed water level and the simulated water level under NAT and HUM at Xingzi, and (b) the remotely sensed and the simulated lake water occurrence.

With respect to the reservoir impact, for 2013–2022, the streamflow at Yichang (Datong) decreases by 12.4% (6.8%) in the flood season (June to October), increases by 29.1% (11.4%) in the dry season (November to May), and increases by 0.8% (0.5%) annually. For the other 8 hydrologic stations, the streamflow decreases by 0.6%–16.7% in the flood season, and increases by 2.9%–36.7% in the dry season, with minor changes at annual scales. In general, the impact of reservoir operation on the annual streamflow is minor but tends to increase the dry-season streamflow and decrease the flood-season streamflow, with the reservoir impacts gradually intensifying over the periods 1991–2000, 2001–2012, and 2013–2022.

With respect to the impact of irrigation and water withdrawal (in Figure 8), for 2013–2022, the streamflow at Yichang (Datong) decreases by 3.6% (4.6%) in the flood season, decreases by 6% (2.8%) in the dry season, and decreases by 4.3% (3.8%) annually. For the other 8 stations, the streamflow decreases by 1.7%–5.7% in the flood season, by 3.7%–9.3% in the dry season, and by 2.4%–6% annually. Generally, irrigation and water withdrawal reduce streamflow during both the dry and flood seasons.

4.6. Human-Induced Alterations of Extreme Floods

Figure 9 shows the maximum annual flood peaks at Yichang under NAT, RES, and HUM for 1991–2022, and the human-induced alterations of flood peaks for 2013–2022. The maximum annual flood peak at Yichang shows an increasing trend by 159 m³/s per year under NAT, but changes to a decreasing trend by ~250 m³/s per year under both RES and HUM, respectively (Figure 9a). With the construction of reservoirs in the YRB over the last decades, reservoirs attenuate the flood peak at Yichang to an increasing extent, by 4.3% for 1991–2012 to 18% for 2013–2022 (Figure 9c). Reservoir operation is also found able to delay the annual maximum flood peak, with details shown in Text S2 in Supporting Information S1. By further incorporating irrigation and water withdrawal, the maximum annual flood peak is decreased by another 2.4% and 2.8% averaged over 1991–2012 and 2013–2022, respectively.

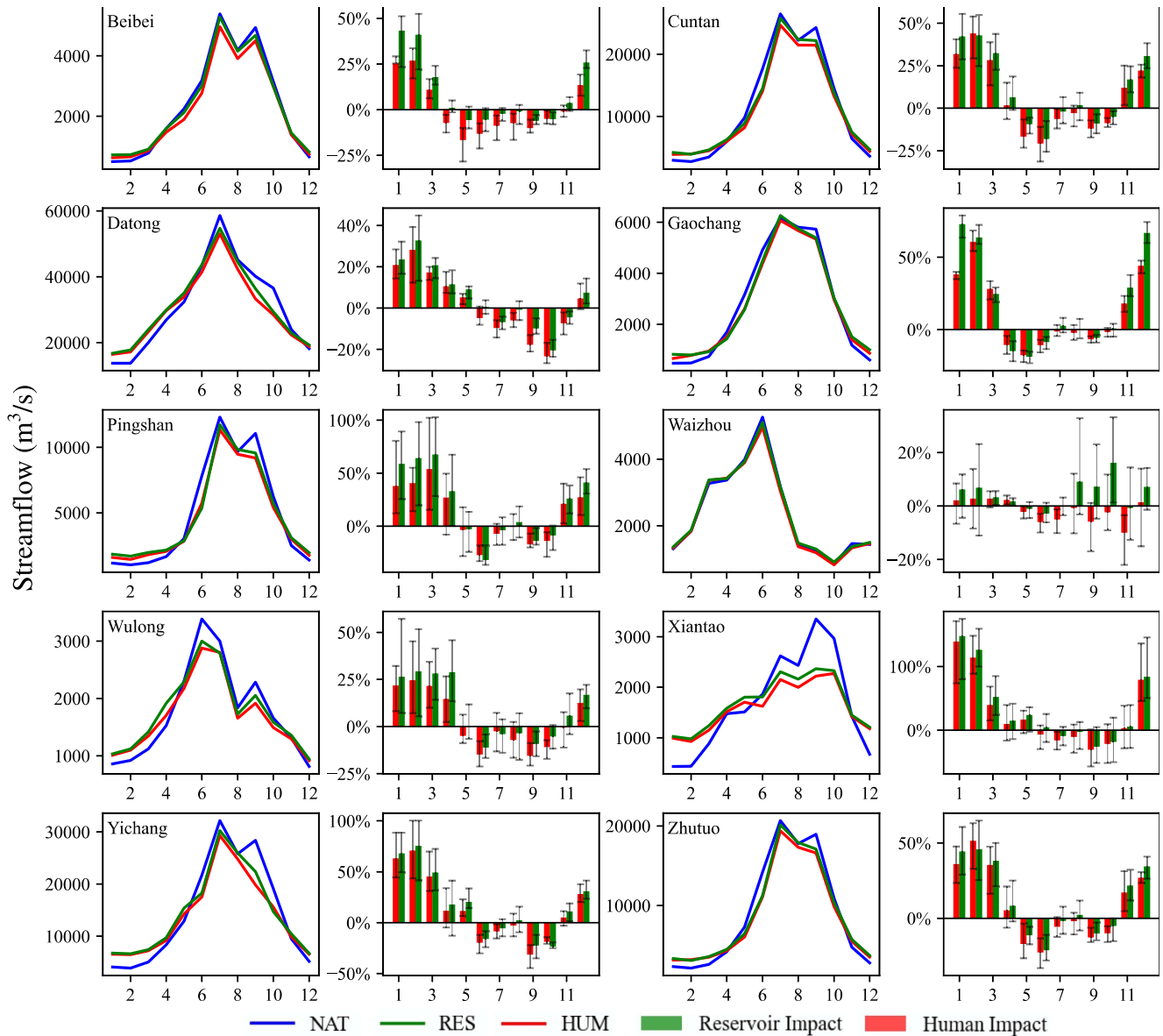


Figure 8. The simulated monthly streamflow and its relative difference due to human activities at 10 hydrologic stations during 2013–2022. Error bars represent 10–90 percentile interval of reservoir and human impacts.

For 2013–2022, the average reduction of the annual maximum flood peak due to reservoir operation accounts for about 89% of that due to the total human activities. This is especially the case for extreme floods, for example, during the record-breaking flood on 20 August 2020, reservoir operation reduces the flood peak at Yichang from 78,220 m³/s to 50,676 m³/s by 35.2%, accounting for over 99% of the total impact of human activities. Note that the observed and simulated flood peak discharges are 50,831 m³/s and 50,551 m³/s, respectively, with a relative error is –0.5%, indicating that the model is able to well reconstruct this extreme flood.

Figure 10 shows the maximum annual flood peak at Datong and its difference under the three scenarios for 2013–2022. Similarly, reservoirs reverse the increasing trend of maximum annual flood peaks (from 336 m³/s to –830 m³/s per 10 years), with the median flood peak decreasing from 63,806 m³/s to 58,635 m³/s for 2013–2022. By further considering irrigation and water withdrawal, the flood peak can be reduced by another 2323 m³/s, to 56,312 m³/s (Figures 10a and 10b).

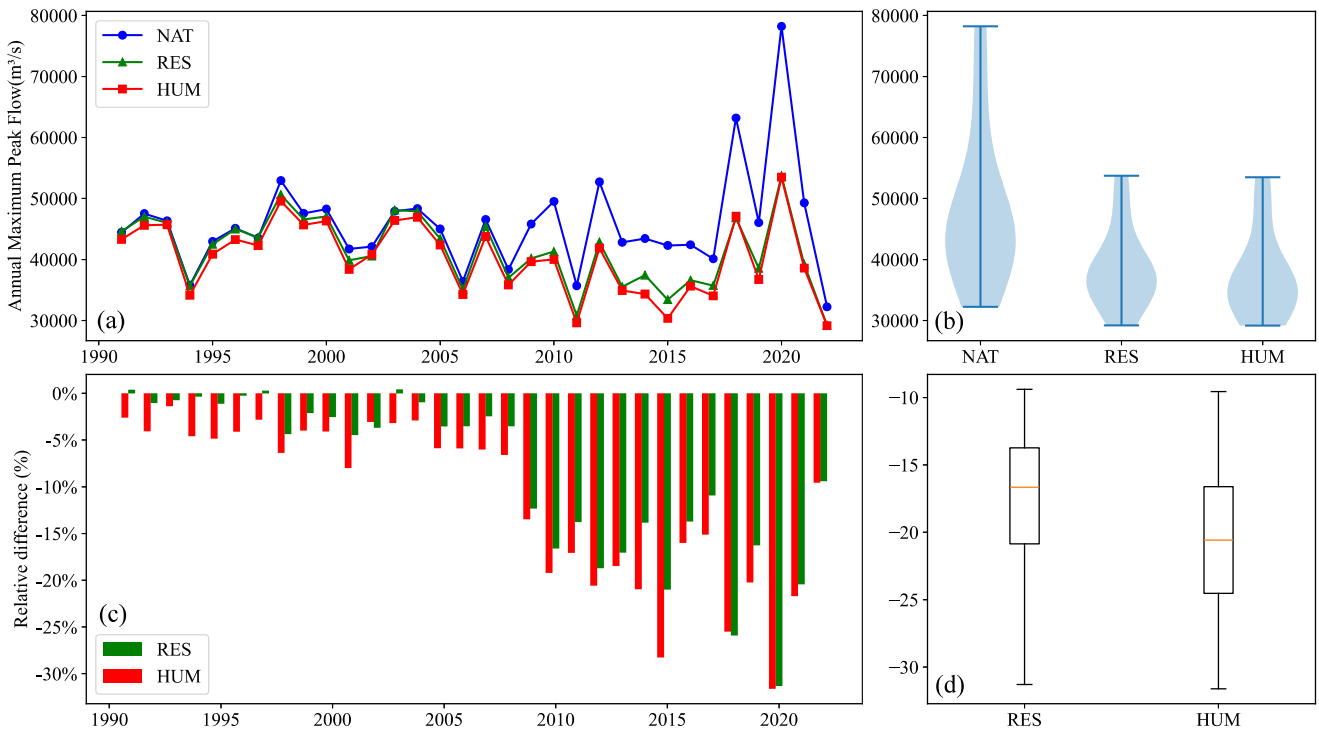


Figure 9. (a) The simulated annual maximum flood peak under three scenarios for 1991–2022 and (b) its variability for 2013–2022; (c) the relative difference of the annual maximum flood peak due to human activities for 1991–2022 and (d) its variability for 2013–2022 at Yichang.

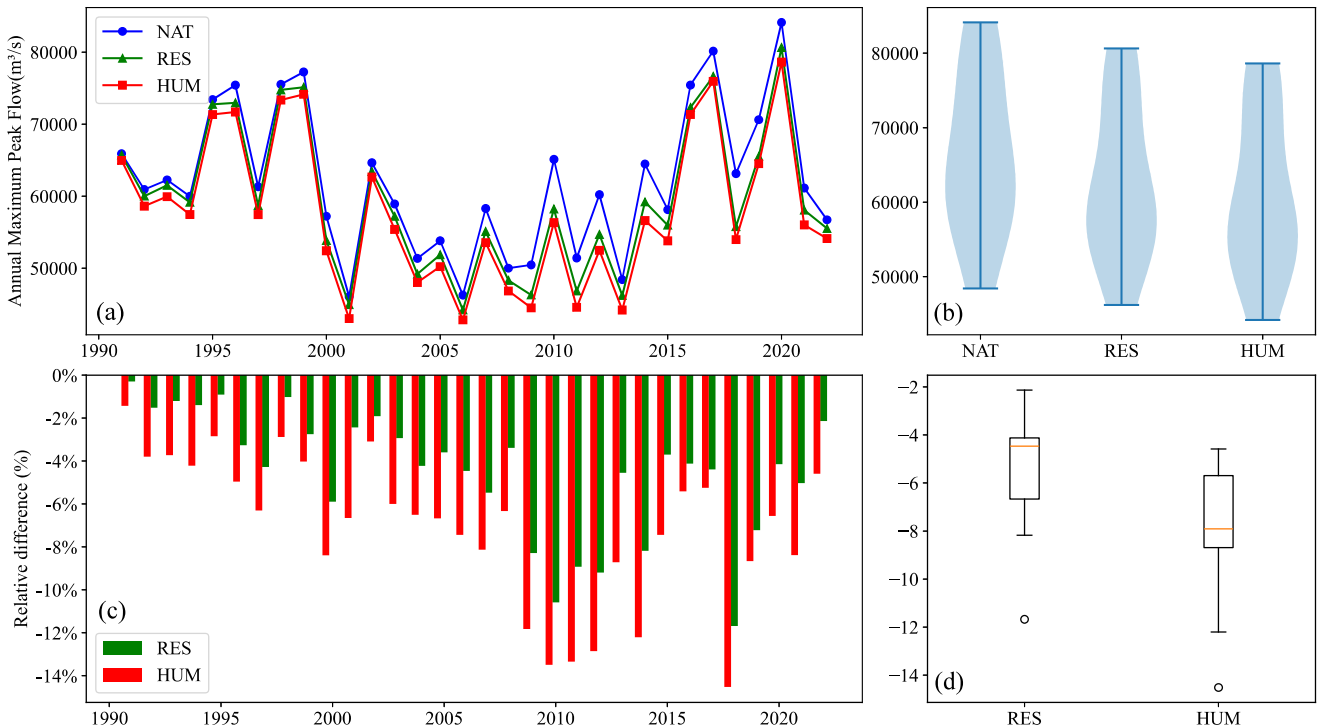


Figure 10. As in Figure 9 but for Datong.

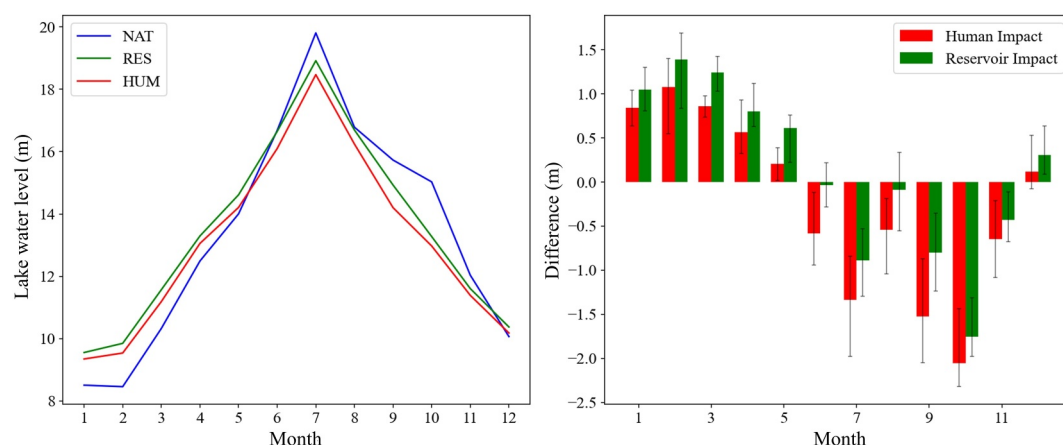


Figure 11. The simulated monthly water level during 2013–2022 (left) and its difference due to human activities (right). Error bars represent 10–90 percentile interval of reservoir and human impacts.

For 2013–2022, the reservoir-induced reduction of maximum flood peaks at Datong is about 5.5%, whereas the reduction by irrigation and water withdrawal is of a similar magnitude, standing at 2.7%. This suggests that irrigation and water withdrawal have a non-negligible impact on the flood peak at Datong (Figures 10c and 10d). A more detailed analysis on the impact of human activities on the flood volume, peak and duration is provided in Text S3 in Supporting Information S1.

4.7. Human-Induced Water Level and Storage Variations of the Poyang Lake

The human-induced lake water level and storage variations are quantified over three periods, namely 1991–2000, 2001–2012, and 2013–2022. Figure 11 illustrates the impact of human activities on the lake water level during 2013–2022, with the impacts for the other two periods in Text S4 in Supporting Information S1.

With respect to the reservoir impact, for 2013–2022, the water level at Xingzi decreases by 0.71 m in the flood season (June to October), whereas it increases by 0.71 m in the dry season (November to May) and by 0.12 m annually. Similarly, the flood-season water storage decreases by 1.26 billion m^3 , whereas the dry-season and annual storage increases by 1.19 billion m^3 and 0.17 billion m^3 , respectively (Figure S8 in Supporting Information S1). In general, the reservoir impacts gradually strengthen over the periods of 1991–2000, 2001–2012, and 2013–2022.

With respect to the impact of irrigation and water withdrawal, for 2013–2022, the water level at Xingzi decreases by 0.49 m in the flood season, decreases by 0.28 m in the dry season, and decreases by 0.37 m annually. Similarly, the flood-season water storage decreases by 1.03 billion m^3 , and the dry-season and annual water storage decrease by 0.39 billion m^3 and 0.66 billion m^3 on average (Figure S8 in Supporting Information S1), respectively. In general, the irrigation and water withdrawal reduce water level and storage during both the dry and flood seasons.

5. Discussion

5.1. Divergent Role of Reservoirs and Irrigation in Flood Mitigation

It is well recognized that both reservoir operation and human water withdrawals can reduce streamflow and also the flood peak, but their respective contributions remain under debate. Results in Section 4.6 indicate that, during 2013–2022, the average reduction of the annual maximum flood peak due to reservoir operation in Yichang accounts for about 89% of that due to the total human activities, far greater than the 11% due to irrigation and water withdrawal. The small contribution to flood peak reduction of irrigation and water withdrawal can be explained by the fact that significant precipitation during extreme floods reduce the irrigation water demand (Zhang, Liu, et al., 2019; Zhang, Wang, & Niu, 2019), thus diminishing the impact of irrigation on floods.

On the other hand, the irrigation plays a much stronger role in mitigating the floods at Datong compared to Yichang. The multi-year average peak flow reduction due to reservoir operation at Datong is only slightly greater than that due to irrigation and water withdrawal, with a ratio of about 6.5:3.5, far lower than the 9:1 at Yichang.

This finding indicates that, whereas the overall mitigating impact of reservoirs on extreme floods exceeds that of irrigation and water withdrawal, their relative contribution is case-dependent. The irrigation and water withdrawal have a more prominent flood mitigating impact at Datong, and the possible reason is the spatial mismatch between the flood origination and the intensive irrigation water demand. The annual maximum flood at Datong often originates from the upper basin (above Yichang) during July and August, whereas during the same period the main flood season in the lower basin (between Yichang and Datong) either has ended or has not started (Figure 8). Therefore, the relatively less precipitation in the lower basin, plus one-third of the annual irrigation water demands occurring during July and August, leads to a significant amount of irrigation water withdrawal and thus a much stronger role in mitigating annual maximum floods. This finding underscores the interacting effects of reservoir operation and irrigation water withdrawal in alleviating the downstream flood damage.

5.2. Altered Lake Hydrodynamics Under Human Activities and Its Ecological Implications

Water level and its fluctuation are crucial to the wetland ecosystem, and have a strong impact on the productivity, species diversity and wetland aquatic plant communities. Our results in Figure 11 indicate that both reservoir operation and irrigation and water withdrawal can reduce the water level at Xingzi at the end of the flood season (September and October) for 2013–2022. Human activities lower the water level by 1.79 m at Xingzi (~16% of the natural annual amplitude of lake water level), with 1.28 m reduction by reservoir operation and 0.51 m reduction by irrigation and water withdrawal. Our findings are generally consistent with the data analysis studies of Chen et al. (2020) and Liu et al. (2017). They reported that the average water level at Xingzi at the end of the flood season decreased by 1.28–1.58 m after the operation of the TGD, which is slightly lower than our finding of 1.79 m. This discrepancy can be explained by the fact that, in our study, 132 reservoirs in addition to the TGD are included to calculate the impacts. Besides, their analyses are based on observed data before and after the operation of the TGD, which may not fully distinguish the impacts of climate change and various human activities, such as the increasing water withdrawal.

The PYL serves as the wintering ground for 95% of the white cranes (Luo, 2014), and is home to the largest migratory goose populations around the globe. The primary aquatic plant in the wetlands of the PYL, *Vallisneria spiralis* (VN), plays a crucial role in feeding waterbirds, oxygenating the water, reducing nutrients, and maintaining ecological balance (Gu et al., 2017; Jiao et al., 2021; Zhu et al., 2016). Chen et al. (2020) found that there is a non-linear relationship between the water level at the end of flood season and the habitat area of VN (Chen et al., 2020), and on the basis of this relationship, we analyze the human-induced impacts on the habitat area of VN. As can be seen in Table S3 in Supporting Information S1, reservoir operation significantly increases the minimum habitat area by 84.4%, while irrigation and water withdrawal decrease it by 9.2%. This suggests that reservoir operation help maintain the VN habitats during the extreme dry years. Furthermore, reservoir operation and human water withdrawal can stabilize the annual variability in the habitat area for VN by 26.8%. This finding clarifies how reservoir operation and human water withdrawal jointly affect the water level at the PYL, emphasizing the importance of water resources management on the lake water level and the wetland ecosystem.

It should be noted that human activities may also impact the hydrodynamics of the PYL in two other ways. First, the construction of upstream reservoirs in the YRB can reduce the sediment loads, leading to clearer water flow that may cause riverbed incision and alter the water level (Gao et al., 2014). Second, there were frequent sand mining activities in the PYL before 2020, which could lower the lakebed elevation and also alter the water level (Yao et al., 2019). The above two aspects are not considered in the model. However, these impacts are considered relatively minor, as the model shows good simulation performance for water level at Xingzi (with the NSE of 0.94). Therefore, subsequent findings can provide implications for understanding the lake hydrodynamics under human impacts.

5.3. Possible Hydrological Impacts of Future Expansion of Irrigated Cropland

According to local water authorities, the irrigated cropland area in the YRB is likely to expand further in the future, making it important to identify potential future hydrologic variations in the basin. In general, future expansion of irrigated cropland can be related to either (a) cropland expanding to areas that are currently not cropland or (b) irrigated cropland expanding to current rain-fed croplands. Due to the fact that the cropland area in the YRB did not increase over recent decades and that most of the land suitable for crop cultivation has been used as cropland (Yuan et al., 2023), we assume that expanding irrigated cropland to current rain-fed cropland is a more

possible future scenario of irrigation area expansion in the YRB. In fact, expanding irrigation area to rainfed crops is also a common practice in previous studies to project possible irrigation area expansion in the future (Rosa, 2022; Rosa et al., 2020; Schmitt et al., 2022).

Based on the above consideration, we set up two new simulation experiments for the study period of 1991–2022 to analyze the hydrologic impacts of future possible irrigation area expansion: (a) the irrigation area remains constant at the current level of 33.38 million hectares (EXP1); and (b) the irrigation area expands to include all current rainfed cropland, increasing to 63.45 million hectares (EXP2). Despite the remarkable increase (~90%) in the irrigation area, the simulated irrigation water demand sees a relatively small increase of ~10%. This is possibly because regions where rain-fed crops are grown generally receive substantial precipitation, which can largely satisfy the water requirement of current rain-fed crops without irrigation.

By comparing EXP1 and EXP2, the impact of future irrigation area expansion on streamflow and dam storage in the YRB can be quantified. Results indicate that future irrigation expansion can slightly decrease the streamflow of Yichang station, with an average annual decrease of 0.5% (see Figure S9 in Supporting Information S1) and a maximum monthly decrease of ~2% in July. This is similar for Datong station but with a slightly less impact. This finding is consistent with several previous studies on humid regions, for example, Haddeland et al. (2006) reported a 2.3% decrease in streamflow of the Mekong River Basin due to irrigation. In terms of the reservoir water storage (Figure S10 in Supporting Information S1), future irrigation expansion can lead to a minor decrease (~0.7%) in the annual water storage of all reservoirs combined in the YRB. This is likely due to the increased water demand leading to increased reservoir releases, which in turn reduces the storage volume (Equations 8 and 10 in Section 3.3).

Overall, the above analysis indicates that the hydrologic impact of future irrigation expansion is relatively minor in the YRB. This suggests that future expansion of irrigated cropland to rainfed cropland in the YRB, if managed well, is unlikely to cause unsustainable consequences to the hydrological balance at the basin scale. This is consistent with several global quantitative assessments of sustainable irrigation (Rosa et al., 2018; Schmitt et al., 2022), which show that current and future irrigation practices are mostly sustainable across the YRB. A quantitative analysis on the sustainability of irrigation expansion, however, is out of the scope of this study.

5.4. Source of Uncertainties and Future Improvements

In this study, the model exhibits a satisfactory accuracy in reconstructing observed streamflow, extreme floods and water level of the PYL, and our results are generally in good agreement with the findings of existing literature. However, our simulation is subject to a few sources of uncertainties that should be taken care of.

Firstly, while the reservoir operation parameters for 90 reservoirs are calibrated against observed data, the reservoir inflow is simulated by the model and is prone to model errors, which can impact the accuracy of reservoir operation simulations. To enhance these inflow simulations, it is advisable to apply more sophisticated techniques such as parameter optimization and regionalization approaches (Gou et al., 2020). Another source of error stems from the simplification of the reservoir operation scheme in our models. Real-time decision-making on dam releases typically takes into account hydrological forecasts, expert experience, and other frequently updated information, all of which can introduce uncertainties into the reservoir operation simulations (Huang, Hejazi, et al., 2018; Huang, Long, et al., 2018; Li et al., 2019; Wu et al., 2018; Yang et al., 2019).

Secondly, the crop growth statuses in the irrigation scheme are based on static data; however, crop growth statuses may vary across years, which could introduce uncertainties in the simulation of irrigation water withdrawals. For example, the time-varying observations such as the greenness vegetation fraction (Nie et al., 2018) can be employed to describe the temporal variability of growth statuses for improved simulation accuracy. This will be one of our future research directions.

Thirdly, to ensure the model computational efficiency, this study employs the 5 km grid resolution and terrain information, which may differ from the actual high-resolution terrain and introduce uncertainties in the simulated hydrodynamics between the mainstream of the Yangtze River and the PYL. To balance the computational speed and the hydrodynamic modeling accuracy, the state-of-the-art global river routing model CaMa-Flood introduced subgrid river and floodplain topography parameters to represent floodplain inundation as a subgrid-scale process (Chaudhari & Pokhrel, 2022; Yamazaki et al., 2011). This could be applied to the CLHMS and other models to achieve higher-resolution hydrodynamic modeling results with relatively coarse native model resolution.

Regardless of these uncertainties, the model validation results suggest that the enhanced model can generally serve as a useful tool to reproduce the observed streamflow, extreme floods and hydrodynamics of the PYL, and subsequent findings can provide insights into the interaction between the human society and the natural hydrological system of the YRB.

6. Conclusions

In this study, we enhance the national-scale coupled land surface-hydrologic-hydrodynamic model (CLHMS) by developing a dynamic irrigation scheme for distinct crops, an extended reservoir operation scheme incorporating both water storage anomalies and water demand anomalies, and a cost-function-based approach to link water demands with reservoir operation. Three controlled simulation experiments are set up to quantify the impacts of anthropogenic activities and their respective components on the hydrological and hydrodynamical variations of the YRB. Major conclusions are highlighted as follows:

1. The enhanced model performs well in simulating the reservoir storage and the irrigation water demand. For the largest 24 reservoirs that account for half of the total capacity of all reservoirs in the YRB, the median NSE of simulated daily water storage stands at 0.67, with a median correlation coefficient of 0.85. The annual irrigation water demands reach an R^2 of 0.8 with published statistics, with a relative error of 1%.
2. The hydrological and hydrodynamical simulations are improved by coupling reservoir operation, irrigation and water withdrawal. The NSE of streamflow at 10 hydrological stations increases from -1.78 – 0.91 to 0.0 – 0.96 for 2013–2022. Flood and lake water level simulations also show a satisfactory accuracy.
3. Reservoir operation, irrigation and water withdrawal have temporally and spatially varying impacts on the streamflow. During 2013–2022, reservoirs increase the flow by 2.9%–36.7% in the dry season, and decrease the flow by 0.6%–16.7% in the flood season, while irrigation and water withdrawal decrease the flow by 2.8%–9.3% in the dry season, and by 1.7%–5.7% in the flood season. The annual flow experiences minor variations under reservoir operation, but reduces by 2.4%–6% under irrigation and water withdrawal.
4. Reservoir operation, irrigation and water withdrawal all reduce flood peak flows, volumes, and duration, but their relative contributions are case-dependent. At the basin scale, the increasing trend of extreme flood peaks exhibits a reversal under human activities, with the flood mitigation effect of irrigation and water withdrawal accounting for up to 50% of that of reservoir operation.
5. Reservoir operation, irrigation and water withdrawal significantly lower the water level and storage of the PYL at the end of the flood season, impacting the aquatic ecological environment. Human activities lower the water level by 1.79 m at Xingzi, with 1.28 m reduction by reservoir operation and 0.51 m reduction by irrigation and water withdrawal.

This study performs a coupled land surface-hydrologic-hydrodynamic modeling analysis, with anthropogenic activities being taken into account. Future work will further couple this model with atmospheric models to explore the human-induced variations in the atmospheric-terrestrial hydrological cycle.

Data Availability Statement

The modeling data and codes used to generate the analyses and the figures are provided in Hao and Dong (2024), deposited at <https://doi.org/10.5281/zenodo.11064829>.

References

- Abbott, B. W., Bishop, K., Zarnetske, J. P., Minaudo, C., Chapin III, F. S., Krause, S., et al. (2019). Human domination of the global water cycle absent from depictions and perceptions. *Nature Geoscience*, 12(7), 533–540. <https://doi.org/10.1038/s41561-019-0374-y>
- Abeshu, G. W., Tian, F., Wild, T., Zhao, M., Turner, S., Chowdhury, A. K., et al. (2023). Enhancing the representation of water management in global hydrological models. *Geoscientific Model Development Discussions*, 2023(18), 1–41. <https://doi.org/10.5194/gmd-16-5449-2023>
- Álamos, N., Alvarez-Garretón, C., Muñoz, A., & González-Reyes, Á. (2024). The influence of human activities on streamflow reductions during the megadrought in central Chile. *Hydrology and Earth System Sciences*, 28(11), 2483–2503. <https://doi.org/10.5194/hess-28-2483-2024>
- Alcamo, J., Döll, P., Henrichs, T., Kaspar, F., Lehner, B., Rösch, T., & Siebert, S. (2003). Development and testing of the WaterGAP 2 global model of water use and availability. *Hydrological Sciences Journal*, 48(3), 317–337. <https://doi.org/10.1623/hysj.48.3.317.45290>
- Allen, R. G., Pereira, L. S., Raes, D., & Smith, M. (1998). Crop evapotranspiration-guidelines for computing crop water requirements—FAO irrigation and drainage paper 56.
- Beck, H. E., Van Dijk, A. I., De Roo, A., Dutra, E., Fink, G., Orth, R., & Schellekens, J. (2017). Global evaluation of runoff from 10 state-of-the-art hydrological models. *Hydrology and Earth System Sciences*, 21(6), 2881–2903. <https://doi.org/10.5194/hess-21-2881-2017>
- Brunner, M. I. (2021). Reservoir regulation affects droughts and floods at local and regional scales. *Environmental Research Letters*, 16(12), 124016. <https://doi.org/10.1088/1748-9326/ac36f6>

Acknowledgments

Ningpeng Dong received funding for this study through the National Key Research and Development Program of China (2023YFC3081000) and the National Natural Science Foundation of China (42401053). Jianhui Wei is supported financially by the German Federal Ministry of Science of Education (BMBF) through funding of the MitRiskFlood project (01LP2005A) and the KARE_II project (01LR2006D1).

- Chao, B. F., Wu, Y. H., & Li, Y. S. (2008). Impact of artificial reservoir water impoundment on global sea level. *Science*, *320*(5873), 212–214. <https://doi.org/10.1126/science.1154580>
- Chaudhari, S., & Pokhrel, Y. (2022). Alteration of river flow and flood dynamics by existing and planned hydropower dams in the Amazon River basin. *Water Resources Research*, *58*(5), e2021WR030555. <https://doi.org/10.1029/2021WR030555>
- Chen, B., Han, M. Y., Peng, K., Zhou, S. L., Shao, L., Wu, X. F., et al. (2018). Global land-water nexus: Agricultural land and freshwater use embodied in worldwide supply chains. *Science of the Total Environment*, *613*, 931–943. <https://doi.org/10.1016/j.scitotenv.2017.09.138>
- Chen, L., Chen, L., Xu, Y., Luan, Z., Jin, Q., Shi, Y., & Hu, T. (2020). Effect of water level change on potential habitat area of bittergrass in Poyang Lake. *Advances in Water Science*, *31*(3). (in Chinese).
- Chen, Y., Niu, J., Kang, S., & Zhang, X. (2018). Effects of irrigation on water and energy balances in the Heihe River basin using VIC model under different irrigation scenarios. *Science of the Total Environment*, *645*, 1183–1193. <https://doi.org/10.1016/j.scitotenv.2018.07.254>
- Dang, H., & Pokhrel, Y. (2024). Evolution of river regimes in the Mekong River basin over 8 decades and the role of dams in recent hydrological extremes. *Hydrology and Earth System Sciences*, *28*(14), 3347–3365. <https://doi.org/10.5194/hess-28-3347-2024>
- Darlane, A. B., & Pouryafar, E. (2021). Quantifying and projection of the relative impacts of climate change and direct human activities on streamflow fluctuations. *Climatic Change*, *165*(1–2), 34. <https://doi.org/10.1007/s10584-021-03060-w>
- Devanand, A., Huang, M., Ashfaq, M., Barik, B., & Ghosh, S. (2019). Choice of irrigation water management practice affects Indian summer monsoon rainfall and its extremes. *Geophysical Research Letters*, *46*(15), 9126–9135. <https://doi.org/10.1029/2019gl083875>
- Döll, P., Hoffmann-Dobrev, H., Portmann, F. T., Siebert, S., Eicker, A., Rodell, M., et al. (2012). Impact of water withdrawals from groundwater and surface water on continental water storage variations. *Journal of Geodynamics*, *59*, 143–156. <https://doi.org/10.1016/j.jog.2011.05.001>
- Dong, N., Wei, J., Yang, M., Yan, D., Yang, C., Gao, H., et al. (2022). Model estimates of China's terrestrial water storage variation due to reservoir operation. *Water Resources Research*, *58*(6), e2021WR031787. <https://doi.org/10.1029/2021wr031787>
- Dong, N., Yang, M., Wei, J., Arnault, J., Laux, P., Xu, S., et al. (2023). Toward improved parameterizations of reservoir operation in ungauged basins: A synergistic framework coupling satellite remote sensing, hydrologic modeling, and conceptual operation schemes. *Water Resources Research*, *59*(3), e2022WR033026. <https://doi.org/10.1029/2022wr033026>
- Flörke, M., Kynast, E., Bärlund, I., Eisner, S., Wimmer, F., & Alcamo, J. (2013). Domestic and industrial water uses of the past 60 years as a mirror of socio-economic development: A global simulation study. *Global Environmental Change*, *23*(1), 144–156. <https://doi.org/10.1016/j.gloenvcha.2012.10.018>
- Gao, J. H., Jia, J., Kettner, A. J., Xing, F., Wang, Y. P., Xu, X. N., et al. (2014). Changes in water and sediment exchange between the Changjiang River and Poyang Lake under natural and anthropogenic conditions, China. *Science of the Total Environment*, *481*, 542–553. <https://doi.org/10.1016/j.scitotenv.2014.02.087>
- Gao, P., Mu, X. M., Wang, F., & Li, R. (2011). Changes in streamflow and sediment discharge and the response to human activities in the middle reaches of the Yellow River. *Hydrology and Earth System Sciences*, *15*(1), 1–10. <https://doi.org/10.5194/hess-15-1-2011>
- Garcia, M., Ridolfi, E., & Di Baldassarre, G. (2020). The interplay between reservoir storage and operating rules under evolving conditions. *Journal of Hydrology*, *590*, 125270. <https://doi.org/10.1016/j.jhydrol.2020.125270>
- Gong, L., Xu, C. Y., Chen, D., Hallidin, S., & Chen, Y. D. (2006). Sensitivity of the Penman–Monteith reference evapotranspiration to key climatic variables in the Changjiang (Yangtze River) basin. *Journal of Hydrology*, *329*(3–4), 620–629. <https://doi.org/10.1016/j.jhydrol.2006.03.027>
- Gonzalez, J. M., Olivares, M. A., Medellin-Azuara, J., & Moreno, R. (2020). Multipurpose reservoir operation: A multi-scale tradeoff analysis between hydropower generation and irrigated agriculture. *Water Resources Management*, *34*(9), 2837–2849. <https://doi.org/10.1007/s11269-020-02586-5>
- Gou, J., Miao, C., Duan, Q., Tang, Q., Di, Z., Liao, W., et al. (2020). Sensitivity analysis-based automatic parameter calibration of the variable infiltration capacity (VIC) model for streamflow simulations over China. *Water Resources Research*, *56*(1), e2019WR025968. <https://doi.org/10.1029/2019wr025968>
- Gou, J., Miao, C., Samaniego, L., Xiao, M., Wu, J., & Guo, X. (2021). CNRD v1. 0: A high-quality natural runoff dataset for hydrological and climate studies in China. *Bulletin of the American Meteorological Society*, *102*(5), 1–57. <https://doi.org/10.1175/bams-d-20-0094.1>
- Gu, Y., Wang, J., Wang, J., Gensheng, F., & Lu, H. (2017). Morphological response and growth strategy of the submerged macrophyte *Vallisneria spiralis* L. under different water depths. *Journal of Lake Sciences*, *29*(3), 654–661. (in Chinese). <https://doi.org/10.18307/2017.0314>
- Guo, H., Hu, Q., Zhang, Q., & Feng, S. (2012). Effects of the three gorges dam on Yangtze River flow and river interaction with Poyang Lake, China: 2003–2008. *Journal of Hydrology*, *416*, 19–27. <https://doi.org/10.1016/j.jhydrol.2011.11.027>
- Haddeland, I., Lettenmaier, D. P., & Skaugen, T. (2006). Effects of irrigation on the water and energy balances of the Colorado and Mekong river basins. *Journal of Hydrology*, *324*(1–4), 210–223. <https://doi.org/10.1016/j.jhydrol.2005.09.028>
- Hanasaki, N., Kanae, S., & Oki, T. (2006). A reservoir operation scheme for global river routing models. *Journal of Hydrology*, *327*(1–2), 22–41. <https://doi.org/10.1016/j.jhydrol.2005.11.011>
- Hanasaki, N., Yoshikawa, S., Pokhrel, Y., & Kanae, S. (2018). A global hydrological simulation to specify the sources of water used by humans. *Hydrology and Earth System Sciences*, *22*(1), 789–817. <https://doi.org/10.5194/hess-22-789-2018>
- Hao, H., & Dong, N. (2024). Data and codes [Dataset]. *Zenodo*. <https://doi.org/10.5281/zenodo.11064829>
- Huang, Q., Long, D., Du, M., Zeng, C., Li, X., Hou, A., & Hong, Y. (2018). An improved approach to monitoring Brahmaputra River water levels using retracked altimetry data. *Remote Sensing of Environment*, *211*, 112–128. <https://doi.org/10.1016/j.rse.2018.04.018>
- Huang, Z., Hejazi, M., Li, X., Tang, Q., Vernon, C., Leng, G., et al. (2018). Reconstruction of global gridded monthly sectoral water withdrawals for 1971–2010 and analysis of their spatiotemporal patterns. *Hydrology and Earth System Sciences*, *22*(4), 2117–2133. <https://doi.org/10.5194/hess-22-2117-2018>
- IEA. (2024). *Monthly electricity statistics [Dataset]*. International Energy Agency (IEA).
- Janssen, M., Lennartz, B., & Wöhling, T. (2010). Percolation losses in paddy fields with a dynamic soil structure: Model development and applications. *Hydrological Processes: International Journal*, *24*(7), 813–824. <https://doi.org/10.1002/hyp.7525>
- Jiao, J., Shi, K., Li, P., Sun, Z., Chang, D., Shen, X., et al. (2018). Assessing of an irrigation and fertilization practice for improving rice production in the Taihu Lake region (China). *Agricultural Water Management*, *201*, 91–98. <https://doi.org/10.1016/j.agwat.2018.01.020>
- Jiao, Y., Yuan, Q., Wang, W., Yan, L., Mu, X., Li, H., & Zhang, S. (2021). *Vallisneria spiralis* tolerance and response of microbial community in wetlands to excess nutrients loading. *Ecological Indicators*, *131*, 108179. <https://doi.org/10.1016/j.ecolind.2021.108179>
- Joseph, J., & Ghosh, S. (2023). Representing Indian agricultural practices and paddy cultivation in the variable infiltration capacity model. *Water Resources Research*, *59*(1), e2022WR033612. <https://doi.org/10.1029/2022wr033612>
- JRC. (2016). Global surface water [Dataset]. *Joint Research Center (JRC)*. <https://global-surface-water.appspot.com/download>
- Kärsdotter, E., Destouni, G., Ghajarnia, N., Lammers, R. B., & Kalantari, Z. (2022). Distinguishing direct human-driven effects on the global terrestrial water cycle. *Earth's Future*, *10*(8), e2022EF002848. <https://doi.org/10.1029/2022ef002848>

- Kebede, E. A., Oluoch, K. O. A., Siebert, S., Mehta, P., Hartman, S., Jägermeyr, J., et al. (2024). *A global open-source dataset of monthly irrigated and rainfed cropped areas (MIRCA-OS) for the 21st century*. HydroShare. Retrieved from <http://www.hydroshare.org/resource/c6d6aacc640de4b0881aa83132990d2b2>
- Leng, G., Huang, M., Tang, Q., Gao, H., & Leung, L. R. (2014). Modeling the effects of groundwater-fed irrigation on terrestrial hydrology over the conterminous United States. *Journal of Hydrometeorology*, *15*(3), 957–972. <https://doi.org/10.1175/jhm-d-13-049.1>
- Leng, G. Y., Leung, L. R., & Huang, M. Y. (2017). Significant impacts of irrigation water sources and methods on modeling irrigation effects in the ACME Land Model. *Journal of Advances in Modeling Earth Systems*, *9*(3), 1665–1683. <https://doi.org/10.1002/2016ms000885>
- Li, B., Yang, G., Wan, R., Lai, X., & Wagner, P. D. (2022). Impacts of hydrological alteration on ecosystem services changes of a large river-connected lake (Poyang Lake), China. *Journal of Environmental Management*, *310*, 114750. <https://doi.org/10.1016/j.jenvman.2022.114750>
- Li, X., Long, D., Huang, Q., Han, P., Zhao, F., & Wada, Y. (2019). High-temporal-resolution water level and storage change data sets for lakes on the Tibetan Plateau during 2000–2017 using multiple altimetric missions and Landsat-derived lake shoreline positions. *Earth System Science Data*, *11*(4), 1603–1627. <https://doi.org/10.5194/essd-11-1603-2019>
- Li, Y., Zhao, G., Allen, G. H., & Gao, H. (2023). Diminishing storage returns of reservoir construction. *Nature Communications*, *14*(1), 3203. <https://doi.org/10.1038/s41467-023-38843-5>
- Liang, J., Yi, Y., Li, X., Yuan, Y., Yang, S., Li, X., et al. (2021). Detecting changes in water level caused by climate, land cover and dam construction in interconnected river–lake systems. *Science of the Total Environment*, *788*, 147692. <https://doi.org/10.1016/j.scitotenv.2021.147692>
- Lin, P., Pan, M., Beck, H. E., Yang, Y., Yamazaki, D., Frasson, R., et al. (2019). Global reconstruction of naturalized river flows at 2.94 million reaches. *Water Resources Research*, *55*(8), 6499–6516. <https://doi.org/10.1029/2019wr025287>
- Liu, H., Zheng, L., Jiang, L., & Liao, M. (2020). Forty-year water body changes in Poyang Lake and the ecological impacts based on Landsat and HJ-1 A/B observations. *Journal of Hydrology*, *589*, 125161. <https://doi.org/10.1016/j.jhydrol.2020.125161>
- Liu, X., Liu, W., Yang, H., Tang, Q., Flörke, M., Masaki, Y., et al. (2019). Multimodel assessments of human and climate impacts on mean annual streamflow in China. *Hydrology and Earth System Sciences*, *23*(3), 1245–1261. <https://doi.org/10.5194/hess-23-1245-2019>
- Liu, Z., Guo, S., Guo, J., & Liu, P. (2017). The impact of Three Gorges Reservoir refill operation on water levels in Poyang Lake, China. *Stochastic Environmental Research and Risk Assessment*, *31*(4), 879–891. <https://doi.org/10.1007/s00477-016-1209-7>
- Lo, M. H., & Famiglietti, J. S. (2013). Irrigation in California's Central Valley strengthens the southwestern US water cycle. *Geophysical Research Letters*, *40*(2), 301–306. <https://doi.org/10.1002/grl.50108>
- Luo, W. (2014). *Study on ecohydrological process and regulation countermeasures in typical wetland of Poyang Lake under changing environment*[D]. Wuhan University. (in Chinese).
- Mu, S., Yang, G., Xu, X., Wan, R., & Li, B. (2022). Assessing the inundation dynamics and its impacts on habitat suitability in Poyang Lake based on integrating Landsat and MODIS observations. *Science of the Total Environment*, *834*, 154936. <https://doi.org/10.1016/j.scitotenv.2022.154936>
- Müller Schmied, H., Cáceres, D., Eisner, S., Flörke, M., Herbert, C., Niemann, C., et al. (2021). The global water resources and use model WaterGAP v2. 2d: Model description and evaluation. *Geoscientific Model Development*, *14*(2), 1037–1079. <https://doi.org/10.5194/gmd-14-1037-2021>
- Nie, W., Zaitchik, B. F., Rodell, M., Kumar, S. V., Anderson, M. C., & Hain, C. (2018). Groundwater withdrawals under drought: Reconciling GRACE and land surface models in the United States High Plains Aquifer. *Water Resources Research*, *54*(8), 5282–5299. <https://doi.org/10.1029/2017wr022178>
- Pekel, J. F., Cottam, A., Gorelick, N., & Belward, A. S. (2016). High-resolution mapping of global surface water and its long-term changes. *Nature*, *540*(7633), 418–422. <https://doi.org/10.1038/nature20584>
- Pokhrel, Y., Felfelani, F., Satoh, Y., Boulange, J., Burek, P., Gädeke, A., et al. (2021). Global terrestrial water storage and drought severity under climate change. *Nature Climate Change*, *11*(3), 226–233. <https://doi.org/10.1038/s41558-020-00972-w>
- Pokhrel, Y., Hanasaki, N., Koirala, S., Cho, J., Yeh, P. J. F., Kim, H., et al. (2012). Incorporating anthropogenic water regulation modules into a land surface model. *Journal of Hydrometeorology*, *13*(1), 255–269. <https://doi.org/10.1175/jhm-d-11-013.1>
- Portmann, F. T., Siebert, S., & Döll, P. (2010). MIRCA2000—Global monthly irrigated and rainfed crop areas around the year 2000: A new high-resolution data set for agricultural and hydrological modeling. *Global Biogeochemical Cycles*, *24*(1). <https://doi.org/10.1029/2008gb003435>
- Qin, D., Lu, C., Liu, J., Wang, H., Wang, J., Li, H., et al. (2014). Theoretical framework of dualistic nature–social water cycle. *Chinese Science Bulletin*, *59*(8), 810–820. <https://doi.org/10.1007/s11434-013-0096-2>
- Rosa, L. (2022). Adapting agriculture to climate change via sustainable irrigation: Biophysical potentials and feedbacks. *Environmental Research Letters*, *17*(6), 063008. <https://doi.org/10.1088/1748-9326/ac7408>
- Rosa, L., Chiarelli, D. D., Sangiorgio, M., Beltran-Peña, A. A., Rulli, M. C., D'Odorico, P., & Fung, I. (2020). Potential for sustainable irrigation expansion in a 3 C warmer climate. *Proceedings of the National Academy of Sciences*, *117*(47), 29526–29534. <https://doi.org/10.1073/pnas.2017796117>
- Rosa, L., Rulli, M. C., Davis, K. F., Chiarelli, D. D., Passera, C., & D'Odorico, P. (2018). Closing the yield gap while ensuring water sustainability. *Environmental Research Letters*, *13*(10), 104002. <https://doi.org/10.1088/1748-9326/aadeef>
- Schmitt, R. J., Rosa, L., & Daily, G. C. (2022). Global expansion of sustainable irrigation limited by water storage. *Proceedings of the National Academy of Sciences*, *119*(47), e2214291119. <https://doi.org/10.1073/pnas.2214291119>
- Siebert, S., & Doell, P. (2008). *The global crop water model (GCWM): Documentation and first results for irrigated crops Frankfurt Hydrology paper 07 (42)*. Institute of Physical Geography, University of Frankfurt. (Reprinted).
- Song, L., Song, C., Luo, S., Chen, T., Liu, K., Li, Y., et al. (2021). Refining and densifying the water inundation area and storage estimates of Poyang Lake by integrating Sentinel-1/2 and bathymetry data. *International Journal of Applied Earth Observation and Geoinformation*, *105*, 102601. <https://doi.org/10.1016/j.jag.2021.102601>
- Sutanudjaja, E. H., Van Beek, R., Wanders, N., Wada, Y., Bosmans, J. H., Drost, N., et al. (2018). PCR-GLOBWB 2: A 5 arcmin global hydrological and water resources model. *Geoscientific Model Development*, *11*(6), 2429–2453. <https://doi.org/10.5194/gmd-11-2429-2018>
- Voisin, N., Li, H., Ward, D., Huang, M., Wigmosta, M., & Leung, L. R. (2013). On an improved sub-regional water resources management representation for integration into earth system models. *Hydrology and Earth System Sciences*, *17*(9), 3605–3622. <https://doi.org/10.5194/hess-17-3605-2013>
- Wada, Y., de Graaf, I. E., & van Beek, L. P. (2016). High-resolution modeling of human and climate impacts on global water resources. *Journal of Advances in Modeling Earth Systems*, *8*(2), 735–763. <https://doi.org/10.1002/2015ms000618>
- Wada, Y., Van Beek, L. P. H., Viviroli, D., Dürr, H. H., Weingartner, R., & Bierkens, M. F. (2011). Global monthly water stress: 2. Water demand and severity of water stress. *Water Resources Research*, *47*(7). <https://doi.org/10.1029/2010wr009792>

- Wada, Y., Wisser, D., & Bierkens, M. F. (2014). Global modeling of withdrawal, allocation and consumptive use of surface water and groundwater resources. *Earth System Dynamics*, 5(1), 15–40. <https://doi.org/10.5194/esd-5-15-2014>
- Wagner, S., Fersch, B., Yuan, F., Yu, Z., & Kunstmann, H. (2016). Fully coupled atmospheric-hydrological modeling at regional and long-term scales: Development, application, and analysis of WRF-HMS. *Water Resources Research*, 52(4), 3187–3211. <https://doi.org/10.1002/2015WR018185>
- Wang, L., Peng, Z., Ma, X., Zheng, Y., & Chen, C. (2021). Multiscale gravity measurements to characterize 2020 flood events and their spatio-temporal evolution in Yangtze River of China. *Journal of Hydrology*, 603, 127176. <https://doi.org/10.1016/j.jhydrol.2021.127176>
- Wang, R., Xiong, L., Xu, X., Liu, S., Feng, Z., Wang, S., et al. (2023). Long-term responses of the water cycle to climate variability and human activities in a large arid irrigation district with shallow groundwater: Insights from agro-hydrological modeling. *Journal of Hydrology*, 626, 130264. <https://doi.org/10.1016/j.jhydrol.2023.130264>
- Wang, Z., Yang, Y., Chen, G., Wu, J., & Wu, J. (2021). Variation of lake-river-aquifer interactions induced by human activity and climatic condition in Poyang Lake Basin, China. *Journal of Hydrology*, 595, 126058. <https://doi.org/10.1016/j.jhydrol.2021.126058>
- Wisser, D., Fekete, B. M., Vörösmarty, C. J., & Schumann, A. H. (2010). Reconstructing 20th century global hydrography: A contribution to the global terrestrial network-hydrology (GTN-H). *Hydrology and Earth System Sciences*, 14(1), 1–24. <https://doi.org/10.5194/hess-14-1-2010>
- Wisser, D., Frolking, S., Douglas, E. M., Fekete, B. M., Vörösmarty, C. J., & Schumann, A. H. (2008). Global irrigation water demand: Variability and uncertainties arising from agricultural and climate data sets. *Geophysical Research Letters*, 35(24). <https://doi.org/10.1029/2008gl035296>
- Wu, J., Liu, Z., Yao, H., Chen, X., Chen, X., Zheng, Y., & He, Y. (2018). Impacts of reservoir operations on multi-scale correlations between hydrological drought and meteorological drought. *Journal of Hydrology*, 563, 726–736. <https://doi.org/10.1016/j.jhydrol.2018.06.053>
- Xia, Q., Liu, P., Fan, Y., Cheng, L., An, R., Xie, K., & Zhou, L. (2022). Representing irrigation processes in the land surface-hydrological model and a case study in the Yangtze River Basin, China. *Journal of Advances in Modeling Earth Systems*, 14(7), e2021MS002653. <https://doi.org/10.1029/2021ms002653>
- Xu, X., Chen, F., Barlage, M., Gochis, D., Miao, S., & Shen, S. (2019). Lessons learned from modeling irrigation from field to regional scales. *Journal of Advances in Modeling Earth Systems*, 11(8), 2428–2448. <https://doi.org/10.1029/2018ms001595>
- Xu, Y., Li, J., Wang, J., Chen, J., Liu, Y., Ni, S., et al. (2020). Assessing water storage changes of Lake Poyang from multi-mission satellite data and hydrological models. *Journal of Hydrology*, 590, 125229. <https://doi.org/10.1016/j.jhydrol.2020.125229>
- Yamazaki, D., Kanae, S., Kim, H., & Oki, T. (2011). A physically based description of floodplain inundation dynamics in a global river routing model. *Water Resources Research*, 47(4), W04501. <https://doi.org/10.1029/2010wr009726>
- Yang, S., Yang, D., Chen, J., & Zhao, B. (2019). Real-time reservoir operation using recurrent neural networks and inflow forecast from a distributed hydrological model. *Journal of Hydrology*, 579, 124229. <https://doi.org/10.1016/j.jhydrol.2019.124229>
- Yao, J., Zhang, D., Li, Y., Zhang, Q., & Gao, J. (2019). Quantifying the hydrodynamic impacts of cumulative sand mining on a large river-connected floodplain lake: Poyang Lake. *Journal of Hydrology*, 579, 124156. <https://doi.org/10.1016/j.jhydrol.2019.124156>
- Yassin, F., Razavi, S., Elshamy, M., Davison, B., Sapriza-Azuri, G., & Wheeler, H. (2019). Representation and improved parameterization of reservoir operation in hydrological and land-surface models. *Hydrology and Earth System Sciences*, 23(9), 3735–3764. <https://doi.org/10.5194/hess-23-3735-2019>
- Yin, Z., Ottele, C., Ciaisi, P., Zhou, F., Wang, X., Jan, P., et al. (2021). Irrigation, damming, and streamflow fluctuations of the Yellow River. *Hydrology and Earth System Sciences*, 25(3), 1133–1150. <https://doi.org/10.5194/hess-25-1133-2021>
- Yu, Z., Lakhtakia, M. N., Yarnal, B., White, R. A., Miller, D. A., Frakes, B., et al. (1999). Simulating the river-basin response to atmospheric forcing by linking a mesoscale meteorological model and hydrologic model system. *Journal of Hydrology*, 218(1–2), 72–91. [https://doi.org/10.1016/S0022-1694\(99\)00022-0](https://doi.org/10.1016/S0022-1694(99)00022-0)
- Yu, Z., Pollard, D., & Cheng, L. (2006). On continental-scale hydrologic simulations with a coupled hydrologic model. *Journal of Hydrology*, 331(1–2), 110–124. <https://doi.org/10.1016/j.jhydrol.2006.05.021>
- Yuan, X., Wang, C., Li, B., Wang, W., & Chen, N. (2023). Review of the driving forces and impacts of land use/cover change in the Yangtze River Basin. *Geomatics and Information Science of Wuhan University*, 48(8), 1241–1255.
- Zajac, Z., Revilla-Romero, B., Salamon, P., Burek, P., Hirpa, F. A., & Beck, H. (2017). The impact of lake and reservoir parameterization on global streamflow simulation. *Journal of Hydrology*, 548, 552–568. <https://doi.org/10.1016/j.jhydrol.2017.03.022>
- Zeng, R., Cai, X., Ringler, C., & Zhu, T. (2017). Hydropower versus irrigation—An analysis of global patterns. *Environmental Research Letters*, 12(3), 034006. <https://doi.org/10.1088/1748-9326/aa5f3f>
- Zhan, J., Chen, J., Zhang, W., Han, X., Sun, X., & Bao, Y. (2018). Mass movements along a rapidly uplifting river valley: An example from the upper Jinsha River, southeast margin of the Tibetan plateau. *Environmental Earth Sciences*, 77, 1–18. <https://doi.org/10.1007/s12665-018-7825-4>
- Zhang, X., Liu, P., Xu, C. Y., Gong, Y., Cheng, L., & He, S. (2019). Real-time reservoir flood control operation for cascade reservoirs using a two-stage flood risk analysis method. *Journal of Hydrology*, 577, 123954. <https://doi.org/10.1016/j.jhydrol.2019.123954>
- Zhang, Y., Wang, Y., & Niu, H. (2019). Effects of temperature, precipitation and carbon dioxide concentrations on the requirements for crop irrigation water in China under future climate scenarios. *Science of the Total Environment*, 656, 373–387. <https://doi.org/10.1016/j.scitotenv.2018.11.362>
- Zhang, Z., Chao, B. F., Chen, J., & Wilson, C. R. (2015). Terrestrial water storage anomalies of Yangtze River Basin droughts observed by GRACE and connections with ENSO. *Global and Planetary Change*, 126, 35–45. <https://doi.org/10.1016/j.gloplacha.2015.01.002>
- Zhang, Z., Chen, X., Xu, C. Y., Hong, Y., Hardy, J., & Sun, Z. (2015). Examining the influence of river–lake interaction on the drought and water resources in the Poyang Lake basin. *Journal of Hydrology*, 522, 510–521. <https://doi.org/10.1016/j.jhydrol.2015.01.008>
- Zhang, Z., Jin, G., Tang, H., Zhang, S., Zhu, D., & Xu, J. (2022). How does the three gorges dam affect the spatial and temporal variation of water levels in the Poyang Lake? *Journal of Hydrology*, 605, 127356. <https://doi.org/10.1016/j.jhydrol.2021.127356>
- Zhou, X., Polcher, J., & Dumas, P. (2021). Representing human water management in a land surface model using a supply/demand approach. *Water Resources Research*, 57(4), e2020WR028133. <https://doi.org/10.1029/2020wr028133>
- Zhu, T., Cao, T., Ni, L., He, L., Yi, C., Yuan, C., & Xie, P. (2016). Improvement of water quality by sediment capping and re-vegetation with *Vallisneria spiralis* L.: A short-term investigation using an in situ enclosure experiment in Lake Erhai, China. *Ecological Engineering*, 86, 113–119. <https://doi.org/10.1016/j.ecoleng.2015.10.031>

References From the Supporting Information

- Lang, M., Ouarda, T. B., & Bobée, B. (1999). Towards operational guidelines for over-threshold modeling. *Journal of Hydrology*, 225(3–4), 103–117. [https://doi.org/10.1016/S0022-1694\(99\)00167-5](https://doi.org/10.1016/S0022-1694(99)00167-5)

- Sun, J., Chen, W., Hu, B., Xu, Y. J., Zhang, G., Wu, Y., et al. (2023). Roles of reservoirs in regulating basin flood and droughts risks under climate change: Historical assessment and future projection. *Journal of Hydrology: Regional Studies*, *48*, 101453. <https://doi.org/10.1016/j.ejrh.2023.101453>
- Volpi, E., Di Lazzaro, M., Bertola, M., Viglione, A., & Fiori, A. (2018). Reservoir effects on flood peak discharge at the catchment scale. *Water Resources Research*, *54*(11), 9623–9636. <https://doi.org/10.1029/2018WR023866>
- Wang, X., Lu, J., Chen, X., & Li, Y. (2022). Flood mitigation effects of lake-reservoir group on the Poyang Lake watershed based on runoff-weighted model from multi-satellite weekly observation. *Journal of Hydrology: Regional Studies*, *44*, 101265. <https://doi.org/10.1016/j.ejrh.2022.101265>